Dissecting function and catalytic mechanism of fungal lytic polysaccharide monooxygenases

Bing Liu

Faculty of Natural Resources and Agricultural Sciences

Department of Molecular Sciences

Uppsala

Doctoral thesis
Swedish University of Agricultural Sciences
Uppsala 2019

Acta Universitatis agriculturae Sueciae
2019:43

Cover: Computational simulation of *H. irregulare* LPMO9B binding on cellulose surface

(Modelling: Abhishek A. Kognole)

ISSN 1652-6880
ISBN (print version) 978-91-7760-404-4
ISBN (electronic version) 978-91-7760-405-1

Print: SLU Service/Repro, Uppsala 2019

Dissecting function and catalytic mechanism of fungal lytic polysaccharide monooxygenases (LPMOs)

Abstract

Fungi use a complex and well-orchestrated enzyme machinery to degrade lignocellulose biomass, in which both hydrolytic and redox enzymes are involved. Lytic polysaccharide monoxygenases (LPMOs) are copper-dependent enzymes that cleave bonds in polysaccharides using oxidative mechanisms. LPMOs belonging to auxiliary activity family 9 (AA9) are widely distributed in the fungal kingdom. The aim of this study is to develop a better understanding of the roles of AA9 LPMOs in lignocellulose degradation with the focus on a white-rot softwood-decaying fungus *Heterobasidion irregulare* as well as to gain more insights into their catalytic mechanism by investigating the interaction of C1-specific AA9 LPMOs with substrate/co-substrate at molecular level. Two LPMOs from *H. irregulare (Hi*LPMO9H *and Hi*LPMO9I) were shown to have different substrate specificity against cellulose and glucomannan, indicating that AA9 LPMOs may be involved in degradation of different plant cell wall components during the decay of softwood by the *H. irregulare* (Paper I). Another *H. irregulare* LPMO (*Hi*LPMO9B) was found to increase the substrate accessibility for a homologous cellobiohydrolase (*Hi*Cel7A) and the cooperation between these two enzymes were shown during crystalline cellulose degradation, indicating that AA9 LPMO may act in synergy with cellulases as importance members in the cellulose degradation system of *H. irregulare* (Paper II). Molecular dynamics showed that the C1-specific *Hi*LPMO9B uses acidic residues to bind onto the cellulose surface in addition to hydrophobic residues (Paper III). Furthermore, it was shown that cyanide inhibits the activity of the C1-specific *Pc*LPMO9D by competing with O_2 binding to the enzyme. Cyanide was shown to bind to the axial position of copper coordinating sites, reflecting a possible scenario of the proposed Cu-superoxyl intermediate (Paper IV). The present study has increased our understanding of the functionalization of LPMO in basidiomycete fungi and has expanded the current view on possible substrate/co-substrate interaction at molecular level.

Keywords: lignocellulose, fungi, LPMO, biological role, catalytic mechanism

Author's address: Bing Liu, SLU, Department of Molecular Sciences,
P.O. Box 7015, SE-750 07 Uppsala, Sweden

Dedication

To all those care about me

“Though you seem to have taken a longer way to the goal, you never give up approaching it.”

尽管你看似走了一些弯路，却从未放弃向梦想再近一步。

from a friend of mine.

Contents

List of publications

This thesis is based on the work contained in the following papers, referred to by Roman numerals in the text:

I **Liu, B**., Olson, Å., Wu, M., Broberg, A. & Sandgren, M. (2017). Biochemical studies of two lytic polysaccharide monooxygenases from the white-rot fungus *Heterobasidion irregulare* and their roles in lignocellulose degradation. *PLOS ONE*, 12(12), p e0189479.

II **Liu, B**., Krishnaswamyreddy, S., Muraleedharan, M. N., Olson, Å., Broberg, A., Ståhlberg, J. & Sandgren, M. (2018). Side-by-side biochemical comparison of two lytic polysaccharide monooxygenases from the white-rot fungus *Heterobasidion irregulare* on their activity against crystalline cellulose and glucomannan. *PLOS ONE*, 13(9), p e0203430.

III **Liu, B**., Kognole, A. A., Wu, M., Westereng, B., Crowley, M. F., Kim, S., Dimarogona, M., Payne, C. M. & Sandgren, M. (2018). Structural and molecular dynamics studies of a C1-oxidizing lytic polysaccharide monooxygenase from *Heterobasidion irregulare* reveal amino acids important for substrate recognition. *The FEBS Journal*, 285(12), pp 2225–2242.

IV Forsberg, Z.*, **Liu, B**.*, Åsmund, K. R., Bissaro, B., Eijsink, V. G. H. Sandgren, M. Structural and biochemical study of the effects of cyanide on a fungal lytic polysaccharide monooxygenase (Manuscript). * First authorship shared

Papers I-III are reproduced with the permission of the publishers.

Publications not included in this thesis:

Vuong, T. V., **Liu, B**., Sandgren, M. & Master, E. R. (2017). Microplate-Based Detection of Lytic Polysaccharide Monooxygenase Activity by Fluorescence-Labeling of Insoluble Oxidized Products. *Biomacromolecules*, 18(2), pp 610–616.

The contribution of Bing Liu to the papers included in this thesis was as follows:

I Designed the methods for gene knock-in for heterogeneous protein expression in *P. pastoris*; Performed protein expression, purification and biochemical characterization; Take leading role in data interpretation and paper writing.

II Performed enzyme assays, bioanalytical analysis and structural modeling/comparison; Take leading role in data interpretation and paper writing.

III Performed protein expression, purification; Contributed in structural determination of the enzyme; Took active role in data interpretation and paper writing together with other co-authors.

IV Performed protein expression and purification, Solved the enzyme-ligand structures by X-ray crystallography. Took active role in data interpretation and paper writing together with other co-authors.

Abbreviations

AA	Auxiliary activity
AFM	Atomic force microscopy
BMCC	Bacterial microcrystalline cellulose
CAZy	Carbohydrate-active enzyme
CBM	Carbohydrate binding module
CMC	Carboxymethyl cellulose
CN	Cyanide
EG	Endoglucanase
ESI-MS	Electrospray ionization mass spectrometry
GH	Glycoside hydrolase
HPAEC	High-performance anion exchange chromatography
LPMO	Lytic polysaccharide monoxygenase
NMR	Nuclear magnetic resonance
PASC	Phosphoric acid swollen cellulose
ROS	Reactive oxygen specie

1 Introduction

1.1 Lignocellulosic biomass degradation by fungi

Microorganisms play an important role in the degradation of plant biomass in the biosphere (Mäkelä *et al.*, 2014). It is known that a wide range of microorganisms, including bacteria and fungi, synthesize and secrete enzymes to decompose plant biomass (Guerriero *et al.*, 2015), which is mainly composed of lignocellulose (Bar-On *et al.*, 2018). For decades, lignocellulose-degrading enzymes have been of great interest due to their potential use in industrial applications for biomass conversion into bio-based fuels and chemicals (Jaramillo *et al.*, 2015). It has been known for a long time that the microbial degradation of plant biomass is associated with complex enzymatic machineries with well-orchestrated cooperation between a variety of plant cell wall degrading enzymes. Still many details of the enzyme machinery for degradation of lignocellulosic polysaccharides remains to be elucidated. The discovery of a new class of oxidative enzymes named lytic polysaccharide monoxygenases (LPMOs) has greatly expanded the current understanding on lignocellulose degradation by microorganisms in nature. Accordingly, it is essential to understand the catalytic mechanism and the biological roles of LPMOs, which will not only provide more insights into biological mechanism of wood degradation by microorganisms (Cragg *et al.*, 2015), but also contribute to the improvement in the efficiency of industrial enzyme cocktails used for sustainable bio-refinery processes (Kuhad *et al.*, 2011).

1.1.1 Wood-decaying fungi

Fungi are well-known for their ability to attack and colonize either living plants or dead plant tissues, and to break down woody biomass. The fungal species in the latter category are often referred to "wood rotters" (Schmidt, 2006). Depending on the type of decay, wood-rotting fungi are divided into three classes: white-rot fungi, brown-rot fungi and soft-rot fungi (Schwarze *et al.*, 2000). Soft-rot fungi are mainly found in phyla ascomycota; they normally attack wood in damp environment and introduce cavities on plant cell walls, causing softening effect of wood surfaces (Levy, 1966). White-rot and brown-rot fungi are found within the basidomycota (Goodell *et al.*, 2008). The invasion of brown-rot fungi results in the infected wood cracking into cubical pieces in brown color (Bagley & Richter, 2002). White-rot fungi cause the wood mass turning to be spongy or stringy in white color. White-rot fungi can potentially under appropriate conditions degrade the entire wood structure (Mester *et al.*, 2004).

1.1.2 Structure and composition of plant cell wall

The biomass of plants is predominantly constituted of plant cell wall, which accounts of around 45-65% of plant dry matter (Foster *et al.*, 2010). The building blocks of plant cell wall are polysaccharides (cellulose, hemicellulose and pectin) and lignin. The plant cell wall consists of three layers: the middle lamella, the primary cell wall and the secondary cell wall. The middle lamella forms the outermost layer of plant cell wall between two adjacent cells and consists mostly of pectin. The primary cell wall, which is formed between the middle lamella and the secondary cell wall, is composed of cellulose, hemicellulose and pectin. In addition to cellulose and hemicellulose, the secondary cell wall also contains lignin (Ochoa-Villarreal *et al.*, 2012).

Mature woods are dominated by secondary cell wall, in which the three components, cellulose, hemicellulose and lignin are organized in a complex three-dimensional structure (Figure 1). Cellulose is a long homopolymer built up of β-1,4-linked glucose. Cellulose chains are assembled into microfibrils through a hydrogen bonding network between neighbouring chains, and cellulose microfibrils further aggregate into bundle-like cellulose fibers (Figure 1). Around 80% of the cellulose fibers are highly packed and described as crystalline regions, which are segmented with disordered regions (also referred to the amorphrous area) (Brett, 2000).

Hemicellulose is a group of heterogenous polysaccharides containing pentoses (xylose and arabinose), hexoses (glucose, galactose, mannose and rhamnose) and/or sugar acids (glucuronic acid and galacturonic acid). The most common hemicellulosic polysaccharides in wood cell walls includes xyloglucan, heteroxylan (arabinoxylan and glucuronoxylan), galactomannan and glucomannan. The backbone of hemicellulose in wood are formed by the sugar moieties connected via β-1,4-linkages, and varied modification are found on the side chains of hemicellulose (Figure 1). The composition of wood hemicellulose varies depending on tree species. Normally it contains mostly glucomannan in softwood such as pine and spruce, whereas it is mostly composed of xylan in hardwood such as birch, aspen and oak (Scheller & Ulvskov, 2010; Ochoa-Villarreal *et al.*, 2012). Compared to cellulose, hemicellulose has a lower degree of polymerization and it has a more branched structure (Figure 1). In secondary cell wall, hemicellulose adheres to the surface of cellulose fibrils via hydrogen bonding and cross-links between cellulose fibers (Scheller & Ulvskov, 2010).

Lignin is a branched complex polymer built up by three different phenylpropane-based monomer units, para-coumaryl alcohol, coniferyl-alcohol and sinapyl-alcohol (Figure 1). The lignin matrix fills the space between and interconnect cellulose and hemicellulose, making the entire structure of cell wall rigid (Feofilova & Mysyakina, 2016).

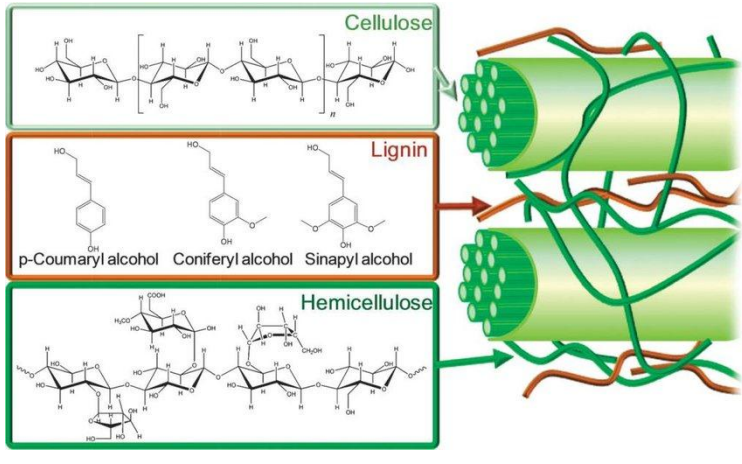

Figure 1. Schematic structure of wood secondary cell wall, illustrated from Alonso et al (2012). The left side of the illustration indicates the chemical composition of three major components of

secondary cell wall (cellulose, hemicellulose and lignin). The right side shows the structural arrangement of those three components in secondary cell wall

1.1.3 Enzymatic hydrolysis of plant cell wall polysaccharides

During fungal colonization on woods, the fungi produce extracellular enzymes that break down the cell wall polysaccharides (e.g. cellulose and hemicellulose) to liberate utilizable sugars. The released sugars are transported into the fungi and hence metabolized. The degradation of cellulose and hemicellulose by fungi involves a complex and well-orchestrated enzyme machinery by synergistic actions of different types of carbohydrate-active enzymes (CAZymes), such as glycoside hydrolases (GHs), carbohydrate esterases (CEs) and redox enzymes (referred to auxilary activity). GH is the largest family of CAZymes and they play essential roles in degradation of polysaccharides by hydrolysis of the linkages between polymerized sugar units (Walker & Wilson, 1991).

The degradation of hemicellulose such as xylan and glucomannan in wood requires a wide range of different enzymes due to the complex composition and structure of the hemicellulose polysaccharides (Figure 2). A variety of debranching enzymes are involved for the removal of side-chain modifications on the xylan backbone, including arabinofuranosidase, glucuronidase, acetylxylan esterase and ferulic acid esterase. Xylanases cleave the backbone of xylan chains to produce shorter xylo-oligosaccharides, which are further converted to xylose by xylosidases (Saha & Bothast, 1999). Similarly, after removal of the galactosyl and acetyl groups on the glucomannan backbone by galactosidase and acetylmannan esterase, a set of endo-acting enzymes introduces internal cleavages on multi-types of linkages of glucomannan backbone. Mannanases mainly cleave β-1,4-mannosidic linkages. While some endoglucanses are able to cleave not only the β-1,4-glucosidic linkages, but also the bonds between a glucosyl and a mannosyl moiety (G-1,4-M or M-1,4-G). The resulting short glucomannan oligosaccharides are further cleaved into monosaccharides (glucose or mannose) by β-1,4-glycosidase or β-1,4-mannosidase (Moreira & Filho, 2008).

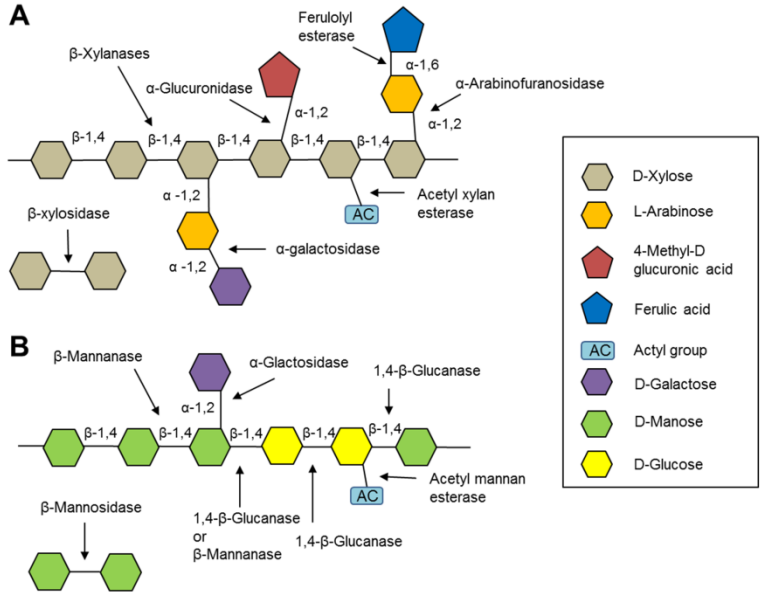

Figure 2. Illustrative presentation on the enzymatic degradation of xylan and glucomannan. Backbone of xylan (**A**) and glucomannan (**B**) with known side chain substitutions are shown, and the activities of enzymes against different bonds in polysaccharides are indicated

The enzymatic degradation of cellulose by fungi was initially described as "Endo-Exo synergism" (Tomme *et al.*, 1995). Processive cellulases such as cellobiohydrolases (CBHs) release cellobiose units from the ends of cellulose chains. Some CBHs proceed from the reducing end while others proceed from the non-reducing end. Endoglucanases cleave the internal glycosidic bonds in amorphous regions, thereby creating more internal free ends for processive enzymes. β-1,4-Glycosidases further convert the produced cellobiose units to glucose (Lynd *et al.*, 2002). The activities of different cellulases are reflected by the structure features (Figure 3).

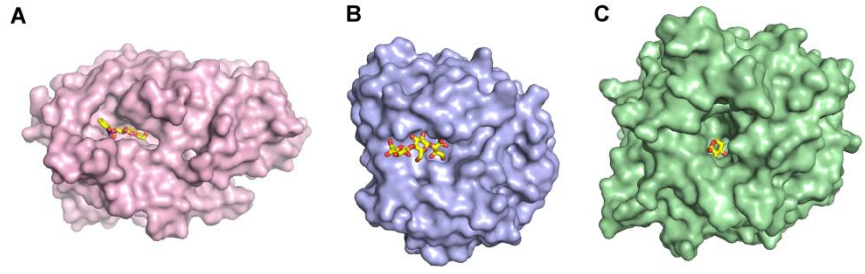

Figure 3. Different active site architectures in cellulose degrading enzymes related to their modes of action. (**A**) Cellobiohydrolases possess a "tunnel" that enable the enzyme to move processively along the cellulose chain (PDB: 4VOE), (**B**) β-1,4-Endoglucanses have a "groove" or "cleft" and are able to cleave bonds internally in long chains (PDB: 1HF6), (**C**) β-1,4-Glycosidases have their active sites in a "pocket" and cleave off residues from one end of oligo- or polysaccharides (PDB: 2JIE). Surface presentation of enzyme structure is shown and bound ligands shown in stick indicate the regions involved in substrate interaction.

1.1.4 Non-hydrolytic factors in cellulose degradation

It has been a question for a long time whether the hydrolysis by glycoside hydrolases is the only type of enzyme activity that occurs in biological cellulose degradation. It is also largely unclear how de-crystallization of cellulose during fungal degradation occurs. In 1950s, It was first proposed that in addition to the hydrolytic activity carried out by glycoside hydrolases, there ought to be a swelling factor (termed C1) that loosens the cellulose crystalline structures and another factor creating more internal sites accessible for cellulases (termed Cx) (Reese *et al.*, 1950). Though the nature and detailed mechanism of the C1 factors still remains unclear, several potential candidates for C1-induced disruption of cellulose crystallinity has been proposed, such as carbohydrate binding modules (CBM), expansins and loosenins (Cosgrove, 1998; Arantes & Saddler, 2010; Quiroz-Castañeda *et al.*, 2011). In the past ten years, enzymes from glycoside hydrolase family 61 (GH61) has drawn extensive interest and research effort. The GH61 enzymes alone are shown to have little activity in cellulose hydrolysis but have considerable stimulating effects on degradation of cellulose when supplemented to canonical cellulases (Harris *et al.*, 2010; Langston *et al.*, 2011). It was initially proposed that the GH61 enzymes potentially could be Cx factors in natural systems. More recent works has shown that GH61 enzymes break the bonds in cellulose using oxidative mechanisms and have therefore been re-categorized into a new

class of enzymes named “lytic polysaccharide monooxygenaes (LPMOs)” (Westereng *et al.*, 2011; Beeson *et al.*, 2012; Li *et al.*, 2012).

1.2 Lytic polysaccharide monoxygenases (LPMOs)

1.2.1 Structure and catalytic mechanism of LPMOs

LPMOs are a class of copper-dependent enzymes that use oxidative mechanisms to cleave bonds in polysaccharides, such as cellulose, hemicellulose, chitin and starch (Vaaje-Kolstad *et al.*, 2010; Westereng *et al.*, 2011; Agger *et al.*, 2014; Leggio *et al.*, 2015). LPMOs have been reported to oxidize either at the C1 or C4 carbon of the glycosidic bonds (Beeson *et al.*, 2012). Most of the current studies supports the idea that the reaction requires an external electron donor and includes a reactive oxygen species such as O_2 as a co-substrate (Hemsworth *et al.*, 2013; Beeson *et al.*, 2015). Although the detailed catalytic mechanism is yet to be fully elucidated, it has been proposed by a quantum mechanical calculation study by Kim *et al.* (2014) that the redox cycle of LPMO reaction starts with the reaction of catalytic copper from Cu (II) to Cu (I) by electron transfer from the external electron donor. Cu (I) binds O_2 to form a Cu (II)-superoxyl complex, which then catalyzes the hydroxylation of the pyranose carbon at either C1 or C4 position on the scissile bond, with two hypotheses that hydroxylation of pyranose carbon could be mediated either via a Cu (II)-superoxyl or Cu (II)-oxyl intermediate by extraction of a proton from one carbon on the glycosidic bond (C1 or C4) and the rebound of a hydroxyl group onto the deprotonated pyranose carbon. According to the quantum mechanism calculation, the Cu (II)-oxyl oxygen rebound mechanism is more energy favorable (Figure 4). The hydroxylation at C1 or C4 results in an unstable intermediate which subsequently decomposes to break the bond between two glycan residues, forming an oxidized end (C1-lactone or C4-ketone) and a native end. In solution, C1-lactone is opened to aldonic acid, and C4-ketone is hydrated to form a gemdiol (Westereng *et al.*, 2011; Isaksen *et al.*, 2014).

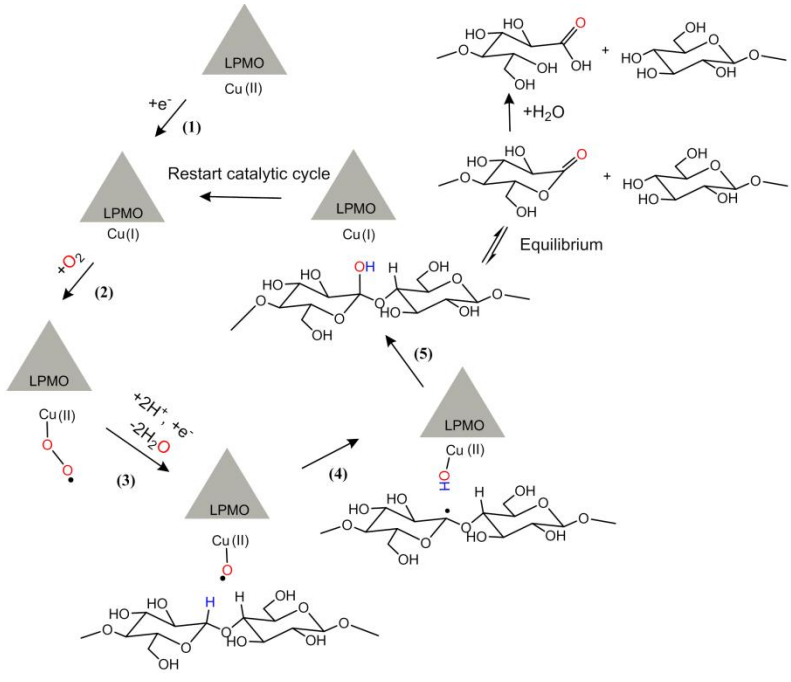

Figure 4. Proposed catalytic mechanism of LPMO using O_2 as co-substrate on cellulose according to Kim et al (2015). The reaction includes several steps: (1) reduction of Cu associated with external electron donation, (2) binding of O_2 to form of Cu(II)-superoxyl complex, (3) formation of Cu(II)-oxyl intermediate associated with external electron donation, (4) Proton extraction by Cu(II)-oxyl intermediate from a carbon of glycosidic bond, (5) hydroxylation of the pyranose carbon.

LPMOs share a similar overall structure with an immuglobin-like β-sandwich fold, with the active site positioned on a nearly flat surface of the protein molecule. The β-sandwich core is composed of two β-sheets that contain 4-5 β-strands respectively. The β-strands are interconnected by loops with or without α-helix insertions (Figure 5A). The active site is a conserved copper-bound motif where the two histidine residues coordinates the catalytic on a plane, and one of the histidine is the N-terminal residue of the mature protein (Figure 5B) (Leggio *et al.*, 2012; Book *et al.*, 2014). Multiple types of ligands like water molecules, peroxide/superoxide ions have been observed in close proximity to the catalytic copper in crystal structures of these enzymes, which is believed to reflect the possible binding scenarios of reactive oxygen species (Li *et al.*, 2012), although there is no yet well-accepted molecular mechanism how the interplay between the reactive oxygen species and the catalytic Cu occurs.

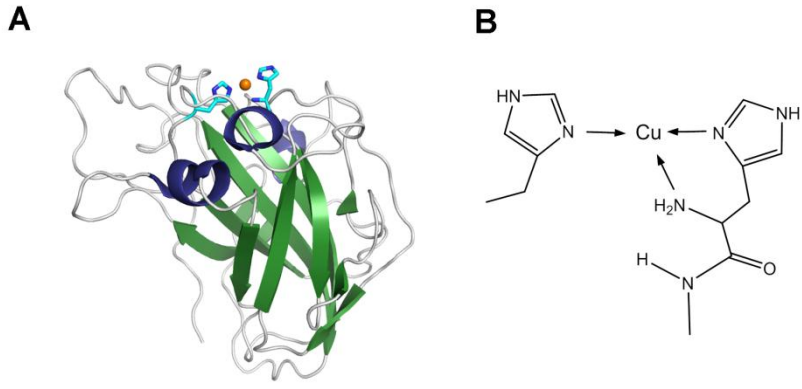

Figure 5. Overall structure and active site of LPMOs. (**A**) An example of a fungal LPMO structure represented by *Neurospora crassa* LPMO9D (PDB: 4EIR). The active site is positioned on a surface with two histidine residues (cyan) coordinating the catalytic Cu (brown) (**B**) Schematic illustration of the conserved motif "histidine brace" around the catalytic copper ion, which is a close-up view of the depicted active site in panel A.

1.2.2 Current classification of LPMOs

LPMOs have been currently divided into six auxiliary activity (AA) families (AA9 AA10, AA11, AA13, AA14 and AA15) based on biological origin, substrate specificity (Table 1) and structural features (Figure 6) in the Carbohydrate-Active enZYmes (CAZy) database (www.cazy.org). AA9 and AA10 are the two largest LPMO families at present, both in terms of the number of putative enzymes and the number of characterized proteins. AA9 LPMOs are only found in fungi, whereas AA10 only found in bacteria. AA9 LPMOs have been found to be active on a wide range of cellulosic and hemicellulosic substrates with varied substrate preferences (Westereng *et al.*, 2011; Agger *et al.*, 2014; Frandsen *et al.*, 2016). Most of the AA10 LPMOs are active on chitin, but some of them also show activity against cellulose (Vaaje-Kolstad *et al.*, 2010; Forsberg *et al.*, 2011). Both AA9 and AA10 have a relatively flat surface, but they show many different features in the surface-exposed loop regions. The most prominent feature is that there is a long loop at C terminal (LC loop) extended from the β-sandwich core of AA9s, which is not observed in AA10s.

So far, only a few LPMOs belonging to the remaining AA families have been identified. These other LPMO containing AA families are separated

from AA9 and AA10 due to the difference in catalytic specificity and structure. AA11 contains fungal LPMOs with activity against chitin. The overall structures of AA11 are similar to AA9. AA11 also have LC loops like AA9 do, but the substrate binding region of AA11 is less flat than that of AA9 (Hemsworth *et al.*, 2014). The AA13 LPMOs are starch-active enzymes of fungal origin. Compared to the rather flat surface of AA9 and AA10, AA13 shows a shallow groove on the substrate binding surface, which is likely to accommodate the α-1,4-linked starch (Leggio *et al.*, 2015). AA14 LPMOs are fungal enzymes with activity against xylan. In contrast to AA9, the surface of AA14 is of rippled shape with a clamp-like motif formed by two surface loops, which is thought to facilitate the binding of a single-chain β-linked polysaccharide, such as xylan (Couturier *et al.*, 2018). The only LPMO belonging to AA15 is found in insects and shows activity against both cellulose and chitin. Unlike LPMOs from other AA families, a unique β-hairpin protrusion close to the active site is observed in AA15, which is thought to be part of substrate binding region of AA15 LPMOs (Sabbadin *et al.*, 2018).

Table 1. Current classification of LPMOs in CAZy database.

LPMO family	Organism	No. of enzyme characterized*	Activity against
AA9	Fungi	39	Cellulose, soluble gluco-oligosaccharides Hemicellulose incl. xyloglucan, glucomannan, mixed β-1-3, 1-4-linked glucan, lichenan, xylan
AA10	Bacteria	21	Chitin or cellulose
AA11	Fungi	2	Chitin
AA13	Fungi	3	Starch
AA14	Fungi	2	Xylan
AA15	Insect	2	Cellulose and chitin

* The number of members in the family where the activity or substrate specificity is known.

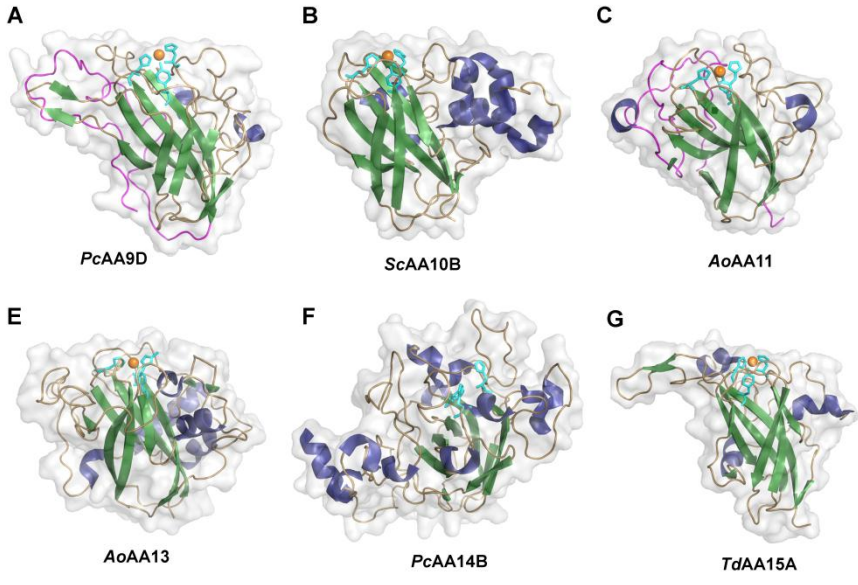

Figure 6. Structural comparison of LPMOs from different auxiliary activity families. (**A**) *Phanerochaete chrysosporium* AA9D active on cellulose (PDB: 4B5Q) (Wu el al, 2013) ; (**B**) *Enterococcus faecalis* AA10A active on chitin (PDB: 4A02) (Vaaje-Kolstad et al, 2011) (**C**) *Streptomyces coelicolor* AA10B active on cellulose (PDB: 4OY6) (Forsberg et al, 2014); (**D**) *Aspergillus oryzae* AA11 active on chitin (PDB: 4MAI) (Hemsworth et al, 2014); (**E**) *Aspergillus oryzae* AA13 active on starch (PDB: 4OPB) (Leggio et al, 2015); (**F**) *Pycnoporus coccineus* AA14B active on xylan (PDB: 5NO7) (Couturier et al, 2018), though no Cu was observed in that crystal structure; (**G**) *Thermobia domestica* AA15 active on cellulose and chitin (PDB: 5MSZ) (Sabbadin et al, 2018). All the crystal structures are visualized in PyMol and colored according to the secondary structure (β-strands: dark green; α-helice: dark blue; loops: light brown). The extended C-terminal loop observed in AA9, AA11 and AA14 is highlighted in magneta. The copper coordinating residues at the active site are shown in cyan. The surface rendition of all LPMO structures is shown in grey with 70% transparency.

1.2.3 Significance of AA9 LPMOs in lignocellulose degradation

The crystallinity of cellulose has been thought to be a huge hindrance of endoglucanase activity and the processivity by cellobiohydrolases (Hall *et al.*, 2010). AA9 LPMOs (previously known as GH61 enzymes) first attracted research interest due to their capability to stimulate the cellulose conversion when included in cellulase cocktails (Harris *et al.*, 2010). Further work revealed that AA9 LPMOs are able to degrade crystalline cellulose into soluble oxidized products (Westereng *et al.*, 2011), and a study using atomic force microscopy (AFM) later demonstrated that AA9

LPMOs are able to make oxidized cleavages on crystalline regions of cellulose surface (Eibinger *et al.*, 2014). Later studies revealed that AA9 LPMOs are able to disrupt the morphology of cellulose fibrillar bundles and separating fibrils from the fibrillar structures, suggesting their importance in the decrystallization of cellulose (Eibinger *et al.*, 2017; Villares *et al.*, 2017). Synergy between LPMOs and cellulases has been shown in several studies, which proposed that AA9 LPMOs increase the substrate accessibility of canonical cellulases on natural lignocellulosic substrates (Jung *et al.*, 2015; Guo *et al.*, 2017; Pierce *et al.*, 2017). This has been further supported by AFM studies showing that binding and digestion efficiency of a processive cellobiohydrolase on crystalline areas of cellulose fibers was enhanced after pretreatment of AA9 LPMOs (Eibinger *et al.*, 2014, 2017). The current understanding in the mechanism of LPMO-cellulase synergy is that AA9 LPMOs create more new chain ends in crystalline areas that can be utilized by progressive cellulases (Figure 7) (Horn *et al.*, 2012; Beeson *et al.*, 2015; Hemsworth *et al.*, 2015; Frommhagen *et al.*, 2018). In addition to the activity against cellulose, AA9 LPMOs have been shown to be active against a variety of hemicellulosic substrates from plant cell wall materials, such as xyloglucan, glucomannan, mixed linkage β-glucan and xylan, suggesting that AA9 LPMOs could contribute to the degradation of different components of plant cell walls (Agger *et al.*, 2014; Bennati-Granier *et al.*, 2015; Frommhagen *et al.*, 2015; Simmons *et al.*, 2017).

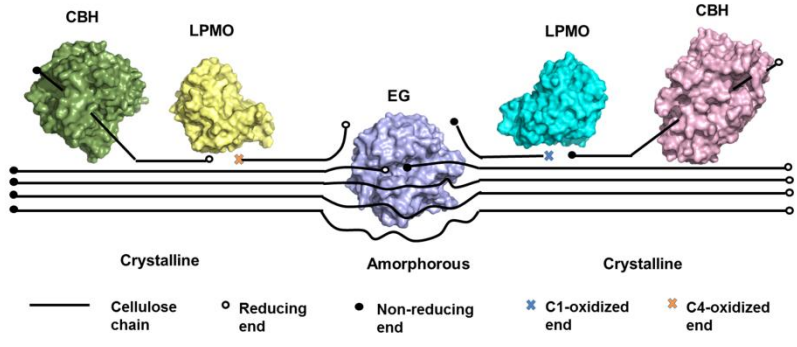

Figure 7. Schematic illustration of the cooperation between LPMOs and known cellulases (EG: endoglucanase and CBH: cellobiohydrolase) in cellulose degradation.

1.2.4 Substrate binding of AA9 LPMOs

The flat surface where the active-site copper is located was preliminarily proposed to be the potential interface for substrate interaction (Karkehabadi *et al.*, 2008). The most variation among the determined AA9 LPMO structures with different substrate specificities are found on the surface exposed loop regions (Loop L2, L3, LS, L8 and LC), suggesting those loop regions may play important roles in substrate binding and substrate selectivity (Leggio *et al.*, 2012). It was first demonstrated using molecular dynamics simulation that three aromatic residues from the surface-exposed loop regions (L2, L3 and LC loop) of C1-specific *Phanerochaete chrysosporium* LPMO9D (*Pc*LPMO9D) contribute significantly to the binding of this enzyme to cellulose chains via hydrophobic interactions (Figure 8A) (Wu *et al.*, 2013). AA9 LPMOs primarily perform C1-oxidization (C1-specific) only showed activities on insoluble cellulose substrates (Westereng *et al.*, 2011; Bennati-Granier *et al.*, 2015; Frommhagen *et al.*, 2016). AA9 LPMOs that are primarily active on C4 (C4-specific) or active on both C1 and C4 (C1/C4-active) display broader substrate preference with activity on both insoluble and soluble substrates, which enable studies of LPMO-substrate interactions using X-ray crystallography and NMR spectroscopy (Agger *et al.*, 2014; Isaksen *et al.*, 2014; Frandsen *et al.*, 2016; Simmons *et al.*, 2017). The first NMR study of a C4-specific AA9 LPMO, *Neurospora crassa* LPMO9C (*Nc*LPMO9C), proved the direct interaction between the β-glucan substrates with the flat catalytic surface of the LPMO (Courtade *et al.*, 2016). Frandsen et al (2016) reported the first crystal structure of a LPMO-substrate complex, in which the cello-oligosaccharide ligands were found bound onto the flat surface of the C1/C4-active *Lentinus similis* LPMO9A (*Ls*LPMO9A) via hydrogen bonding and hydrophobic interaction with residues on the surface-exposed loop regions (L2, L3, L8 and LC loop) (Figure 8B). Crystallographic studies by Simmons et al (2017) further demonstrated the interaction of *Ls*LPMO9A with glucomannan and xylan, which provide further structural insights into the features giving the broad substrate specificity of AA9 LPMOs (Figure 8C, 8D).

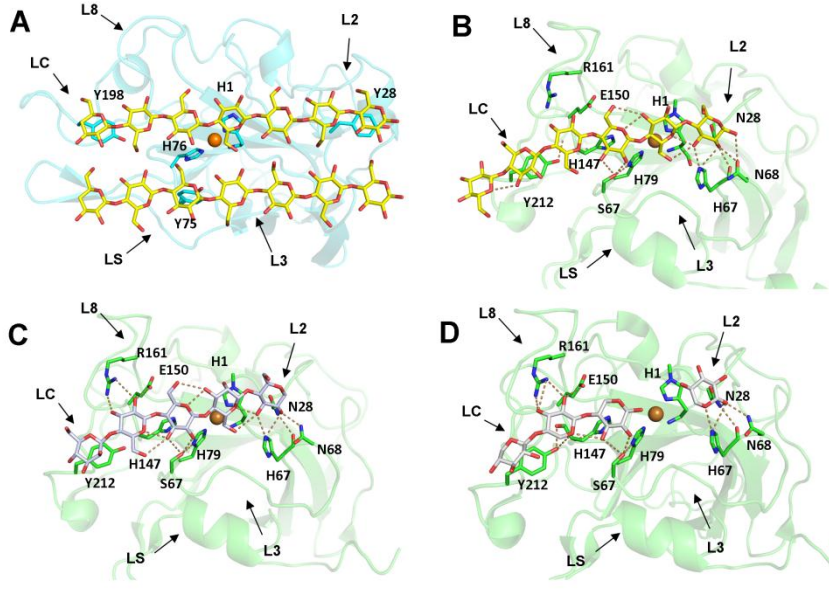

Figure 8. Substrate interaction scenarios of AA9 LPMOs. (**A**) Simulated interaction using molecular dynamics showing *Pc*LPMO9D (cyan) binding onto cellulose surface (yellow carbons) (Wu et al, 2013); (**B**) Crystal structure of *Ls*LPMO9A (green) in complex with cellohexaose (yellow carbons) (PDB: 5ACI); (**C**) Crystal structure where *Ls*LPMO9A (green) binds a glucomannan oligosaccharide (light purple carbons) (PDB: 5NKW); (**D**) Crystal structure in which *Ls*LPMO9A (green) interacts with xylooligosaccharides (light grey carbons) (PDB: 5NLQ). The substrate interacting residues located on the surface-exposed loop regions are shown in sticks and the corresponding loops (L2, L3, L8, LS and LC) are pointed out by arrows.

1.3 Enzyme repertoire of *Heterobasidion irregulare* for cellulose and hemicellulose degradation

The white-rot fungus *Heterobasidion annosum* (Fr.) Bref. *sensu lato* (s.l) is a severe plant pathogen that causes root rot in conifers within the boreal and temperate regions (Asiegbu *et al.*, 2005; Garbelotto & Gonthier, 2013; Lind *et al.*, 2014). *H. annosum* s.l. is a basidiomycete fungal species complex, consisting of five species with distinct phylogeny but partial overlap in geographic distribution and host preferences (Korhonen, 1978; Chase & Ullrich, 1988; Capretti *et al.*, 1990). *H. irregulare* is a native species in North America, and it mainly colonizes and decays softwood trees, such as pine and juniper species (Chase & Ullrich, 1988; Woodward *et al.*, 1998). The invasion cycle of *H. irregulare* on conifer trees is illustrated in Figure 9. This fungus normally infects fresh wood via basidiospores that land on the exposed stump surfaces or injured roots, and spread from one tree to another via root-to-root contacts (Woodward *et al.*, 1998). The mycelia of this fungus grow vertically within the stem of living trees. The infection of *H. irregulare* weakens the health of infected trees and causes damage in the root system, eventually leading to the collapse of the infected tree. *H. irregulare* thereafter continues to degrade the wood of the dead tree. As a severe conifer pathogen, the white-rot fungus *H. irregulare* has been extensively studied at the biological level with the focus on the isolate of *H. irregulare* strain TC 32-1, of which the whole genome have been fully sequenced and annotated (Olson *et al.*, 2012).

Figure 9. Invasion of conifer trees by *H. irregulare* (adapted from the illustration by Jan Stenlid). The cycle includes infection by spores, spread via root contact and colonization on wood.

The *H. irregulare* genome contains 305 putative carbohydrate-active enzymes (Olson *et al.*, 2012). A transcriptomic study revealed that 45 genes from 13 CAzy families are associated with the production of enzymes involved in the degradation of lignocellulose, which include canonical hydrolytic enzymes for degradation of different cell wall polysaccharides such as cellulose, xylan, heteromannan and xyloglucan as well as oxidative enzymes such as LPMOs from family AA9 (Table 2). There are ten AA9 LPMOs encoded in the *H. irregulare* genome (Table 2). The putative AA9 LPMOs from *H. irregulare* ranges in size from 22 to 33 kDa and in isoelectric point (pI) from 4.4 to 6.2. Three of *H. irregulare* LPMOs (*Hi*AA9D, *Hi*AA9H, *Hi*AA9I) are predicted to have a C-terminal CBM1 domain linker to the N-terminal AA9 domain, and the other seven LPMOs contain AA9 domains only (Table 3).

Table 2. Putative enzymes encoded in the genome of *H. irregulare* important for cellulose and hemicellulose degradation (Olson et al, 2012)

CAzy family	Putative function	No. of genes
GH1	β-1,4-Glycosidase	2
GH2	β-1,4-Mannosidase	3
GH5	β-1,4-Endoglucanase or β-1,4-Mannanase	4
GH6	Cellobiohydrolase	1
GH7	Cellobiohydrolase	1
GH9	β-1,4-Glycosidase	1
GH10	β-1,4-Xylanase	2
GH12	β-1,4-Endoglycanse or xyloglucanase	4
GH27	α-Galactosidase	4
GH35	β-Galactosidase	4
GH43	β-Xylosidases or α-Arabinofuranosidase	4
GH45	β-1,4-Endoglucanase	2
GH74	Xyloglucanase	1
AA9	Lytic polysaccharide monooxygenase	10

Table 3. Properties of putative AA9 LPMOs encoded in *H. irregulare* genome (Olson *et al.*, 2012).

Protein ID	Predicted domains	MW (kDa)	pI	NCBI Reference no.
*Hi*AA9A	AA9	22.2	5.0	XP_009550910.1
*Hi*AA9B	AA9	23.8	4.8	XP_009541030.1
*Hi*AA9C	AA9	22.3	4.6	XP_009550870.1
*Hi*AA9D	AA9 + CBM1	31.0	4.4	XP_009552514.1
*Hi*AA9E	AA9	25.0	4.6	XP_009543246.1
*Hi*AA9F	AA9	24.8	5.3	XP_009549038.1
*Hi*AA9G	AA9	22.9	4.2	XP_009546314.1
*Hi*AA9H	AA9 + CBM1	32.5	4.5	XP_009547963.1
*Hi*AA9I	AA9 + CBM1	30.7	4.8	XP_009545898.1
*Hi*AA9J	AA9	32.5	6.2	XP_009549695.1

Global gene expression analysis of *H. irregulare* growing on woody materials revealed that 27 of these 305 protein-encoding genes were up-regulated considerably. Around half of the encoded proteins by the up-regulated genes (14 out of 27) were classified as putative glycoside

hydrolases (GHs) or lytic polysaccharide monooxygenases (LPMOs), indicating the functional importance of those enzymes in lignocellulose degradation (Olson *et al.*, 2012). It was shown that considerable up-regulation of five putative AA9 LPMO genes (*Hi*AA9A, *Hi*AA9B, *Hi*AA9D, *Hi*AA9H and *Hi*AA9I) occurred when the fungus was grown on tree biomass compared to the glucose control (Figure 10), suggesting their importance in lignocellulose degradation. Among the five LPMO genes, both *Hi*AA9H and *Hi*AA9I displayed relatively higher expression levels on pine wood and bark, and both of them contain a C-terminal CBM module; a similar pattern was also observed in *Hi*AA9B, which does not have a CBM attached to the catalytic domain. There are two cellobiohydrolases encoded in *H. irregulare* genome, including one GH7 (*Hi*Cel7A) and one GH6 (*Hi*Cel6A) enzyme. Similar transcriptomic profiles were observed between those *Hi*CBHs and some of the *Hi*LPMOs on plant biomass, which suggests a possible regulated co-expression for cellulose degradation in a potential synergistic mechanism.

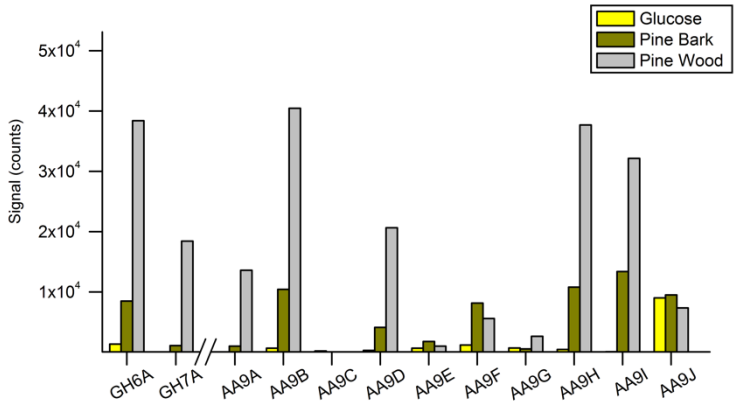

Figure 10. Transcription level of AA9 encoding genes of *H. irregulare* on growth medium with different carbon sources (Olson *et al.*, 2012). The fungus were grown in liquid medium suppliemented with glucose (yellow), homogenates of bark tissue from pine (oliver) or wood shavings of pine (grey). The mRNA expression level of different genes encoding putative enzymes were indicated by the quantification signals in microarray assays.

1.4 Aim of studies

1.4.1 Roles of LPMOs in lignocellulose degradation

The number of AA9 LPMOs encoded in the *H. irregulare* genome raises two questions: **(1)** "*What role(s) do individual AA9 LPMOs play in lignocellulose degradation*" and **(2)** "*How do AA9 LPMOs contribute to the cellulose degradation of H. irregulare*". The first half of this thesis work explores the roles and functions of individual AA9 LPMOs in lignocellulose degradation of white-rot basidiomycete fungus *H. irregulare* by characterizing the substrate specificities and investigating their cooperation with homologous cellulases in cellulose degradation.

1.4.2 Molecular basis of LPMO interaction with substrate and co-substrate

Detailed studies further investigate **(3)** "*How AA9 LPMOs bind on cellulose surface*" and **(4)** "*How the reactive oxygen species is incorporated with the catalytic copper of AA9 LPMOs at the atomic level*", to better understand the catalytic mechanism of LPMOs. Therefore, the second half of this thesis work consists of structure-based characterization to study interaction with substrates such as cellulose as well as co-substrates such as O_2, with the focus on C1-specific LPMOs.

2 Result and Discussion

2.1 The roles of LPMOs in lignocellulose degradation (Paper I & II)

2.1.1 Profiling substrate specificity and regioselectivity of LPMOs in *H. irregulare*

The first characterization study of the AA9 LPMO system of *H. irregulare* was performed by expression and characterization of two CBM1-containing LPMOs, *Hi*LPMO9H and *Hi*LPMO9I (Paper I). The genes encoding *Hi*LPMO9H (GenBank protein accession: AFO72237) and *Hi*LPMO9I (GenBank protein accession: AFO72238) were introduced into the genome of *Pichia pastoris* using CRISPR/Cas9 techniques. Recombinant *Hi*LPMO9H and *Hi*LPMO9I were subsequently expressed in *P. pastoris*. Substrate screening experiments showed that the two enzymes displayed different substrate specificities against cellulosic and hemicellulosic substrates. *Hi*LPMO9I displayed activity against both cellulose and glucomannan, whereas *Hi*LPMO9H only displayed activity on insoluble cellulose among the substrates tested, which included phosphoric acid swollen cellulose (PASC), carboxymethyl cellulose (CMC), cellohexose, xyloglucan, glucomanan, β-1,3-1,4-glucan, β-galactomannan, and glucuronoxylan (Figure 11).

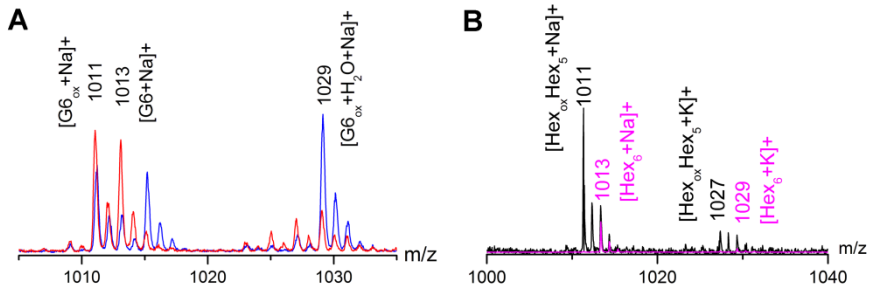

Figure 11. Oxidative cleaving activity of *Hi*LPMO9H and *Hi*LPMO9I on cellulose or glucomannan. (**A**) MALDI-TOF MS analysis indicating the formation of oxidized products (*m/z* -2 or +16 compared to native sugars) after incubating PASC with *Hi*LPMO9H (blue) or *Hi*LPMO9I (red) in presence of ascorbic acid (**B**) MALDI-TOF spectrum showing oxidized products (*m/z* -2 compared to native sugars) generated after the reaction of *Hi*LPMO9I (black) on glucomannan in comparison of the reaction with an GM-active endoglucanse from *Myceliophthora thermophile Mt*EG7 (pink) .

Analysis of the reaction products after treating cellulose substrate with *Hi*LPMO9H and *Hi*LPMO9I by high-performance anion exchange chromatography (HPAEC) revealed that the two enzymes oxidized the product at different positions (Paper I). Only C1-oxidized products (peaks eluted at 19 - 23.8 min) were detected in the reaction products from *Hi*LPMO9H while only C4-oxidized products (22 - 29.5 min on HPAEC chromatogram) were released by *Hi*LPMO9I. It indicated that *Hi*LPMO9H prefer to oxidize at the C1 position of cellulose, whereas *Hi*LPMO9I performs oxidation preliminarily at C4 (Figure 12). Analysis of the reaction products using ESI-MS/MS on oxidized tetra-saccharides, with ions of approximate *m/z* 683.22 confirmed the difference of *Hi*LPMO9H and *Hi*LPMO9I in oxidization preference on cellulose (Figure 12). For *Hi*LPMO9H, two unique ESI-MS/MS product ions (*m/z* 197.0653 and 179.0545) generated from the fragmentation on the ion with *m/z* 683.2230 are in good agreement with the Y_1 fragment ion (*m/z* 197.0656) of aldonic acid cellotetraose and its corresponding ion after elimination of water (Y_1-H_2O, *m/z* 179.0550) (Figure 12A), which supports the C1 oxidization by *Hi*LPMO9H. Fragmentation of the ion with *m/z* 683.2258 from the reaction of *Hi*LPMO9I gave two diagnostic ions (*m/z* 323.0896 and 143.0341), which show good agreement with the fragments B_2-H_2O (*m/z* 323.0973) and B_1-$2H_2O$ (*m/z* 143.0339) from a C4-gemdiol cellotetraose, respectively, and confirmed the C4 oxidization by *Hi*LPMO9I. (Figure 12B).

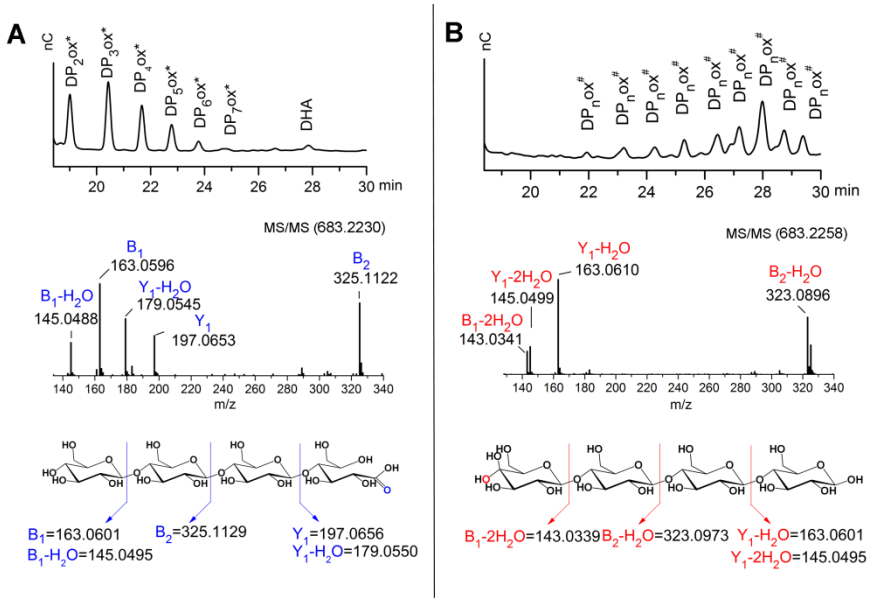

Figure 12. Oxidization preference on cellulose by *Hi*LPMO9H (**A**) and *Hi*LPMO9I **(B)**. Each panel includes a HPAEC analyses of soluble products after incubation of PASC in a zoom-in view to highlight the oxidized sugar region (top) and a MS/MS analysis of oxidized tetra-saccharides with ions of *m/z* 683.22 (middle) compared to the theoretical fragmentation (bottom). DPnox* represents C1-oxdized aldonic sugars. C4-oxidized products are labeled as DPnox#. DHA represents dehydroascorbate.

MS/MS analysis on oxidized oligosaccharides (DP3, DP4 and DP5) produced by *Hi*LPMO9I after incubation with glucomannan indicated that all the oxidized products corresponded to C4-oxidized sugars. (Paper II). The fragmentation of an oxidized tetrasaccharide (*m/z* 700.2503) gave three diagnostic fragment ions [*m/z* 323.09 (B_2-H_2O), 305.08 (B_2-$2H_2O$), 287.07 (B_2-$3H_2O$)], corresponding to B_2 fragment ions of a C4-gemdiol after elimination of water (Figure 13), which supported the specific oxidization preference of *Hi*LPMO9I on the C4 position of sugar moieties in a glucomannan substrate. Further attempts were also made in order to understand which exact bonds in glucomannan are broken by *Hi*LPMO9I (unpublished data). The glucomannan reaction products were subjected to $NaBH_4$ reduction and TFA hydrolysis (Simmons *et al.*, 2017), and the monosaccharide composition was analyzed by HPAEC analysis. Theoretically, oxidative cleavages at the C4 position of the β-1,4-glucosidic linkage (G-1,4-G) would lead to an increase of glucitol and galactose. Instead, the increase of mannitol and galactose occurs when C4 oxidization occurs on the β-D-1,4-pyranosyl linkage between a mannosyl and a glucosyl residue (M-1,4-G); likewise, increase of glucitol and talose corresponding to the C4 oxidization on the bond between a glucosyl and a mannosyl residue (G-1,4-M). HPAEC analyses showed that treatment of *Hi*LPMO9I led to an apparent increase in the level of galactose, glucitol and to a less extent also mannitol, but talose was not detected. These results indicated that *Hi*LPMO9I cleave both the β-D-1,4-pyranosyl linkages between two glucose units (G-1,4-G) and between a mannosyl and a glucosyl residue (M-1,4-G) in glucomannan with specific oxidation preference at the C4 carbon on glucose, but not the β-D-1,4-pyranosyl bonds between a glucosyl and a mannosyl residue (G-1,4-M). Mostly likely, *Hi*LPMO9I has higher activity in cleaving G-1,4-G bonds than M-1,4-G bonds in glucomannan.

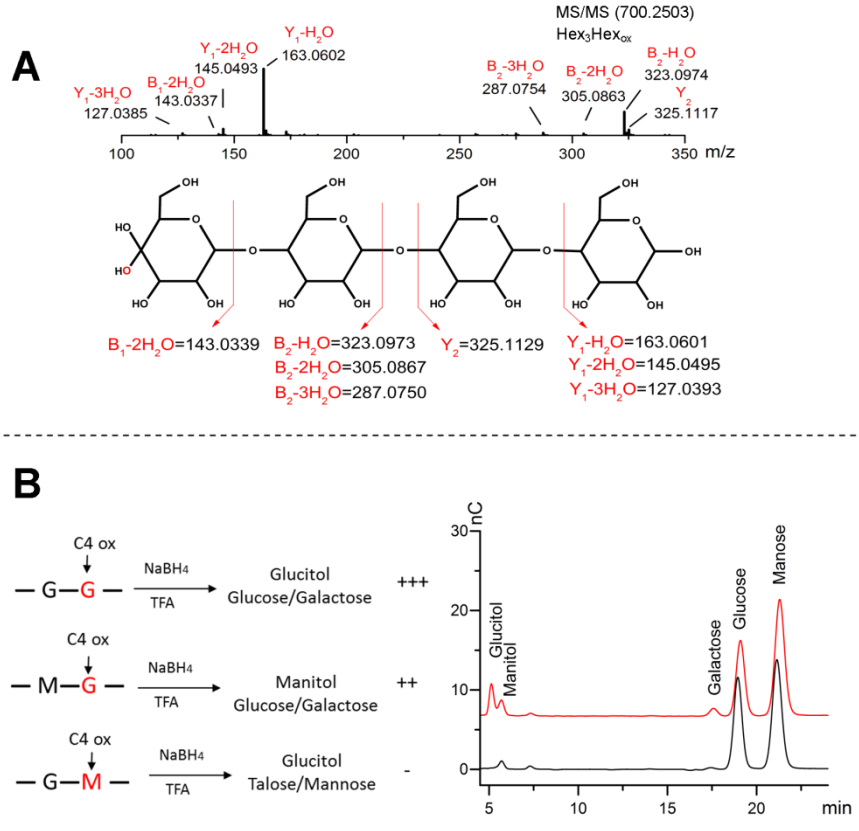

Figure 13. Detailed analysis of regioselectivity of *Hi*LPMO9I on the bonds in konjac glucomannan. (**A**) MS/MS fragmentation of an oxidized tetra-saccharide from the *Hi*LPMO9I-treated glucomannan (upper) and an illustration of theoretical MS/MS fragmentation of a C4-gemidol tetra-saccharide (lower). (**B**) HPAEC-PAD analysis of TFA-hydrolyzed GM products (to the right) after treatment of *Hi*LPMO9I (red) and without LPMO treatment (black). The glucomannan samples were initially reduced using sodium borohydride followed by hydrolysis using triflouroacetic acid (TFA). Possibility of C4 oxidization of different glycosidic bonds and corresponding products are illustrated (Left). The amount of products formed are estimated comparatively based on the observation on HPAEC chromatograms ("+++" highest, "++" middle, "-" lowest or none).

The current studies revealed that AA9 LPMOs from *H. irregulare* have different substrate specificities against plant cell wall polysaccharides. *Hi*LPMO9H is only active on cellulose, while *Hi*LPMO9I is active on both cellulose and glucomannan. Similarly, diversity of substrate specificity of AA9 LPMOs has been reported in several ascomycete fungal systems such as *Neurospora crassa, Podospora anserine and Myceliophthora thermophila* (Beeson *et al.*, 2012; Agger *et al.*, 2014; Bennati-Granier *et al.*, 2015; Frommhagen *et al.*, 2015, 2016). The substrate preference of AA9 LPMOs appeared to correlate with the types of biomass that the fungi colonize in nature. The "bread mold" *Neurospora crassa* displayed activities against polysaccharides that occur abundantly in food crops such as mixed-linkage β-glucan and xyloglucan (Agger *et al.*, 2014). The discovery of AA9 LPMOs that are able to cleave any bonds in xyloglucan in the brown-rot fungi *Gloeophyllum trabeum* and *Fusarium graminearum* correlates with the aptitude of these fungi to degrade hemicellulose (Kojima *et al.*, 2016; Nekiunaite *et al.*, 2016). *Hi*LPMO9I is the LPMO reported so far that is active only on glucomannan among hemicellulose substrates. It corresponds well with the fact that *H. irregular*e decays mainly conifers wood (Woodward *et al.*, 1998), where cellulose and glucomannan are the two major polysaccharides in cell walls (Serin *et al.*, 2003). *Hi*LPMO9I also exhibits capability to relatively strong degrade glucomannan substrates compared to other LPMOs (Paper I and II). This suggests that during the fast colonization that *H. irregulare* on softwood LPMO may be involved in the disruption of glucomannan network, which could potentially facilitate the hyphal penetration across the plant cell walls. Furthermore, the activity on both xylan and glucomannan shown by an AA9 LPMO from the white-rot fungus *Lentinus similis* (*Ls*LPMO9A) correlates with the ability of this fungus to decay both hardwood and softwood (Simmons *et al.*, 2017). In the current study, none of the characterized *H. irregulare* AA9 LPMOs has shown detectable oxidative xylosidic activity. A structural overlay in Paper II suggested that two unique charged residues (an arginine and a glutamic acid) on the L8 loop of xylan/GM-active *Ls*LPMO9A structures are missing in other GM-active LPMOs such as *Hi*LPMO9I and *Nc*LPMO9C, which indicates that these residues are important for AA9 LPMOs to bind both glucomannan and xylan substrates (Simmons *et al.*, 2017). However, AA14 LPMOs have been reported to show activity against xylan, there are two genes encoding putative AA14 enzymes in the genome of *H. irregulare*, *Hi*AA14A (GenBank protein accession: XP_009545121.1) and *Hi*AA14B (GenBank:

XP_009545122.1). Two AA14 LPMOs from the white-rot fungus *Pycnoporus coccineus*, which are 70% identical to the sequences of *Hi*AA14A and *Hi*AA14B, were shown to promote the xylolytic activity of a GH11 xylanase and increase the substrate accessibility of cellulase mixtures on xylan-coated cellulose fibres (Couturier *et al.*, 2018). This suggests that complete degradation of lignocellulosic biomass by *H. irregulare* may involve LPMOs from different families such as AA9 and AA14.

2.1.2 Cooperation between LPMO and cellobiohydrolase in *H. irregulare*

Potential cooperation between a *H. irregulare* CBH I (*Hi*Cel7A) with different types of LPMOs (either *Hi*LPMO9B or *Hi*LPMO9I) when the degradation of crystalline cellulose was investigated using both sequential assays (substrate treated with LPMO first and then CBH) and simultaneous assays (substrate treated with a mixture of LPMO and CBH simultaneously). A clear cooperation was observed between *Hi*LPMO9B and *Hi*Cel7A in saccharification of bacterial microcrystalline cellulose (BMCC), while no cooperation could be detected between *Hi*LPMO9I and *Hi*Cel7A (Paper II). The pretreatment of BMCC with *Hi*LPMO9B led to a significant increase in the total sugar release by *Hi*Cel7A, whereas the pretreatment with *Hi*LPMO9I did not have any effect (Figure 14). Noteworthy, the saccharification level by *Hi*LPMO9B over 48-hour treatment of BMCC (8% of BMCC substrate degraded) was 15 times higher than that shown by *Hi*LPMO9I (0.5% of BMCC substrate degraded) (Figure 15). Though the pretreatment with *Hi*LPMO9B resulted in less insoluble BMCC residues as the substrate for sequential *Hi*Cel7A digestion than the pretreatment with *Hi*LPMO9I, there was still more cello-disaccharides (cellobiose and oxidized cellobiose) released by *Hi*Cel7A with the *Hi*LPMO9B-treated sample. These results indicate that modification of the BMCC substrate by *Hi*LPMO9B makes it more accessible for the degradation by *Hi*Cel7A, whereas *Hi*LPMO9I could not improve the substrate accessibility for *Hi*Cel7A.

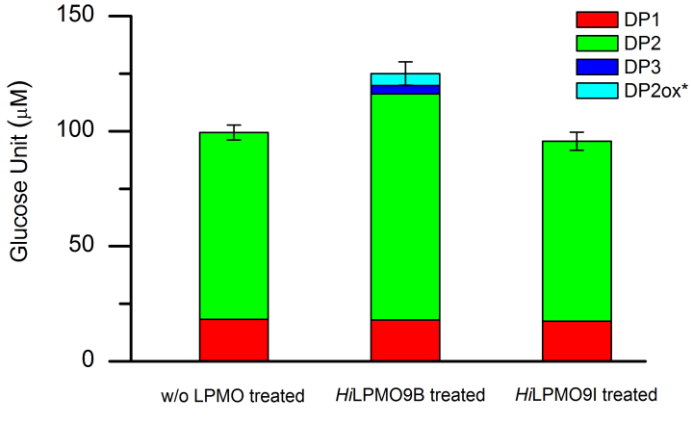

Figure 14. Effects of LPMO pretreatment on *Hi*Cel7A activity against BMCC. The soluble sugars were quantified using HPAEC, and based on 6 h digestion with 0.5 μM *Hi*Cel7A of the BMCC residue after 48 h pretreatment with 0.5 μM *Hi*LPMO9B or *Hi*LPMO9I with 1 mM pyrogallol as reducing agent (LPMO-treated), or with only pyrogallol without LPMO added as negative control (w/o LPMO treatment) at 20 °C, pH 5.0. Each treatment was performed in triplicates. DP1-3 represents glucose, cellobiose and cellotriose; DP2ox* indicates C1-oxidized cellobiose.

The cooperation between *Hi*LPMO9B and *Hi*Cel7A was shown even more clearly in the simultaneous assay, i.e. partial replacement of *Hi*Cel7A with *Hi*LPMO9B gave a considerably higher soluble sugar release compared to using *Hi*Cel7A or *Hi*LPMO9B alone. These results indicate that *Hi*LPMO9B is complementary in activity and cooperate with *Hi*Cel7A in the degradation of cellulose. However, there was practically no stimulation of *Hi*Cel7A by *Hi*LPMO9I. The replacement of *Hi*LPMO9I at all replacement ratios did not lead to significant increase in the overall saccharification level (Figure 15).

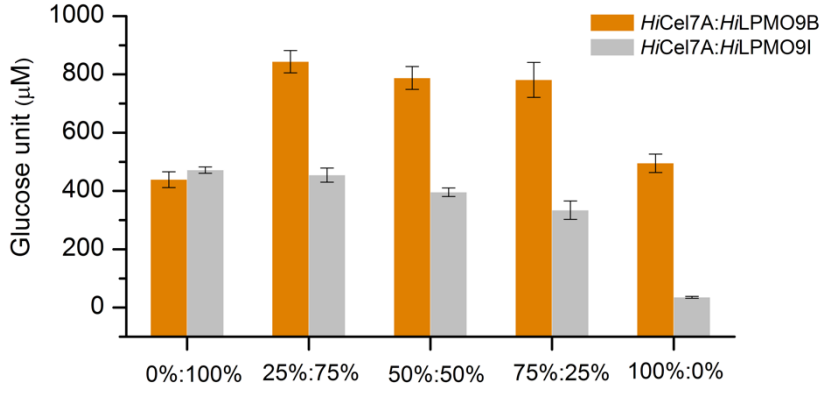

Figure 15. Detected total sugar release using different ratios of mixed *Hi*Cel7A+*Hi*LPMO9B or *Hi*Cel7A+*Hi*LPMO9I. The experiments were performed in simultaneous assays. The total sugar release was quantified by HPAEC based on 48 hr incubation of 1 mg/ml BMCC with 0.5 μM enzyme mixtures of *Hi*Cel7A+*Hi*LPMO9B, or *Hi*Cel7A+*Hi*LPMO9I at 20°C, pH 5.0 in the presence of 1 mM pyrogallol as reducing agent in the experiments of *Hi*Cel7A+*Hi*LPMO9I.

A molecular simulation study on the effects of oxidative cleavage on crystalline cellulose has suggested that the reducing end is always more solvent exposed between the two newly introduced ends at the cleavage site,

no matter whether the oxidization occurs at C1 or C4 (Vermaas *et al.*, 2015). Accordingly, the proposed synergistic effects have been demonstrated by using a reducing-end specific CBH I, *Trichoderma reesei* Cel7A (*Tr*Cel7A), in combination with different AA9 LPMOs. It has been shown that the pretreatment using C1-specific *Nc*LPMO9F boosts the hydrolytic activity of *Tr*Cel7A on Avicel cellulose and the saccharification of crystalline cellulose was significantly accelerated by the addition of C1/C4-active *Tr*LPMO9A to *Tr*Cel7A (Eibinger *et al.*, 2014). At biological level, *Hi*Cel7A is the only GH 7 enzyme encoded in the genome of *H. irregulare*. It is reducing-end specific and contains a single GH7 catalytic domain only (Momeni *et al.*, 2013). It is known from previous studies that when lacking a CBM, GH7 enzymes showed less binding affinity and lower processivity on cellulose (Kont *et al.*, 2016). The current findings showed *Hi*LPMO9B increases the substrate accessibility for reducing end-specific *Hi*Cel7A on cellulose and there is cooperation between *Hi*LPMO9B and *Hi*Cel7A in degradation of crystalline cellulose. Possible explanations could be 1) *Hi*LPMO9B makes C1 oxidized ends on cellulose surface, which creates more new entry points for *Hi*Cel7A's digestion, and 2) *Hi*LPMO9B releases soluble sugar chains from cellulose, which can be more efficiently degraded by *Hi*Cel7A. These also suggest that there is potential synergy between *Hi*Cel7A and *Hi*LPMO9B, and *Hi*LPMO9B may be an important member in the enzyme machinery of *H. irregulare* for cellulose degradation.

On the other hand, the synergistic effects on cellulose degradation have also been reported between LPMOs and CBH II that acts from non-reducing end of crystalline cellulose. A recent report of a C4-specific AA15 LPMO (*Td*AA15A) from the insect *Thermobia domestica*, which is active on both chitin and cellulose, shows clear synergy with a GH6 CBH II when incubated with microcrystalline cellulose (Avicel) (Sabbadin *et al.*, 2018). A preliminary study has been performed to investigate the cooperation of *Hi*Cel6A + *Hi*LPMO9B or that of *Hi*Cel6A + *Hi*LPMO9I (result not published). However, it turned out to be difficult to study a cooperation between a LPMO and *Hi*Cel6A using the current experimental setting, as *Hi*Cel6A is much more efficient in degrading BMCC than *Hi*Cel7A. This could probably be due to the fact that *Hi*Cel6A contains a CBM1 coupled to the GH catalytic domain, which would enable *Hi*Cel6A to be more processive on crystalline cellulose such as BMCC.

2.2 Structural perspectives on cellulose binding and catalytic mechanism of AA9 LPMOs (Paper III & IV)

2.1.3 Cellulose binding of AA9 LPMOs

C1-specific LPMOs have been reported with activity on insoluble cellulose only, suggesting they may play important roles in cellulose degradation. A structural comparison of all hitherto solved C1-specific LPMO structures including the new *Hi*LPMO9B structure, revealed a structural diversity in terms of surface loop regions and the distribution of surface-exposing aromatic residues (Paper III). Different from other currently solved structures of C1-specific AA9 LPMOs, both *Hi*LPMO9B and *Mt*LPMO9G possess an elongated L2 loop. Besides, neither *Hi*LPMO9B nor *Mt*LPMO9G has any aromatic residue located within the L3 loop, compared to other AA9 LPMOs such as *Pc*LPMO9D, *Nc*LPMO9F and *Tt*LPMO9E. Instead, two aromatic residues are found on the elongated L2 loop of these AA9 LPMOs (Figure 16).

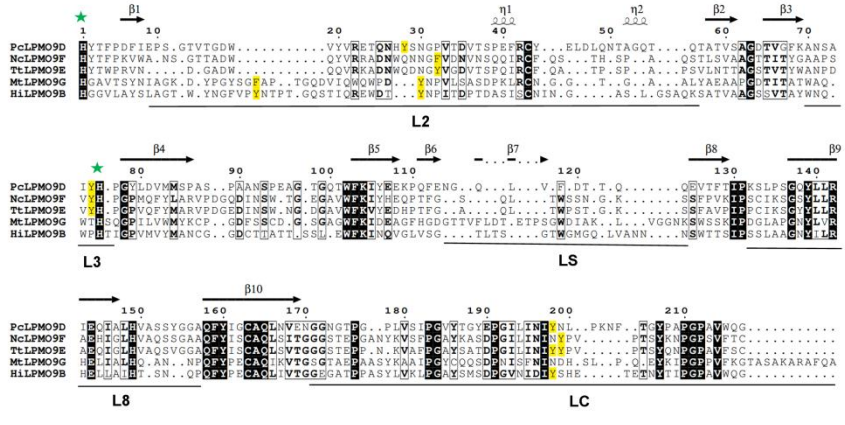

Figure 16. Sequence alignment of C1-specific AA9 LPMOs with known structures, including *Pc*LPMO9D (PDB ID: 4B5Q), *Nc*LPMO9F (PDB ID: 4QI8), *Tt*LPMO9E (PDB ID: 3EJA), *Hi*LPMO9B (PDB ID: 5NNS), *Mt*LPMO9G (PDB ID: 5UFV). The aromatic residues observed on the proposed substrate binding surface of LPMO structures are highlighted in yellow. Residues comprising the active site are labeled with green stars. The secondary structure elements of *Pc*LPMO9D are indicated on the top of the alignment.

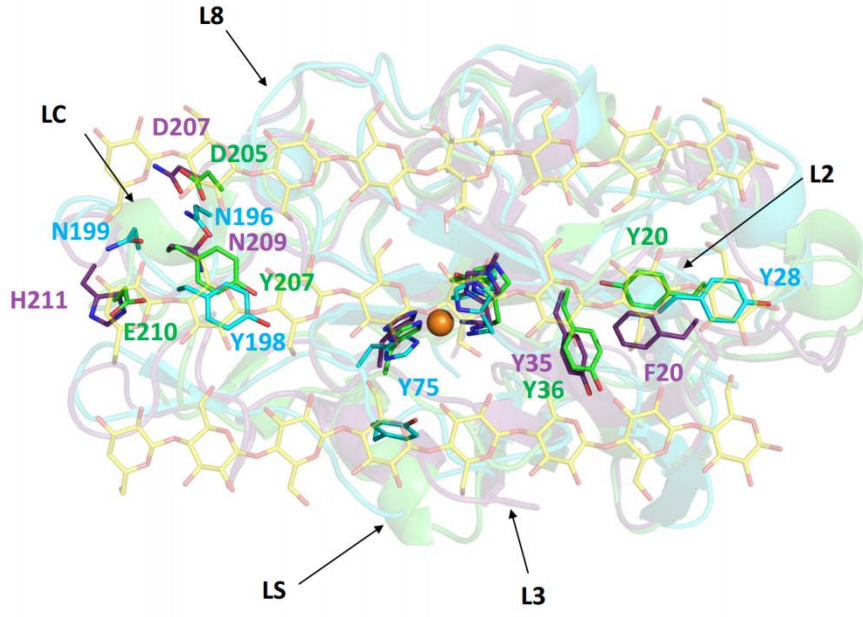

Figure 17. Close-up view of the substrate binding surface after superposition of the *Hi*LPMO9B (green) and *Mt*LPMO9G (dark purple) structures, with the *Pc*LPMO9D (cyan) structure docked on the surface of cellodextrin chains of a cellulose Iβ microfibril (Wu et al, 2013). The proposed substrate interacting residues of *Pc*LPMO9D are shown in cyan sticks, and the residues located in the corresponding positions in *Hi*LPMO9B (green sticks) and *Mt*LPMO9G (dark purple sticks) structure are also shown. The surface exposed loop regions are indicated by arrows.

Previous studies by Wu *et al.*, (2013) showed that regardless of the initial orientation of the LPMO when docked onto a cellulose surface, *Pc*LPMO9D possesses the same binding mode, in which the Tyr-28 from loop L2 and Tyr-198 from loop LC are aligned on the same cellulose chain while Tyr-75 from loop L3 is stacked over the adjacent chain (Figure 17). It was demonstrated using molecular dynamics simulation that the C1-specific LPMO, *Hi*LPMO9B appears to be more flexible in the way of binding onto a cellulose surface (Paper III). These MD studies observed two unique binding modes during the 100-ns duplicated simulation trajectories with three starting points assigned (Figure 18). When *Hi*LPMO9B reached a stabilized binding on the cellulose surface, it was found that the catalytic Cu atom of the LPMO was closer to the C1 carbon than to the C4 carbon of the closest glycosidic bond, and the three tyrosine residues either remained aligned over the same cellulose chain (equilibrium

mode) or rotated to be positioned over three adjacent cellulose chains (rotated mode). During the processes, three surface-exposing tyrosine residues in the *Hi*LPMO9B structure (Tyr-20, Tyr-36 and Tyr-207) were found to be in close contact with the cellulose Iβ surface.

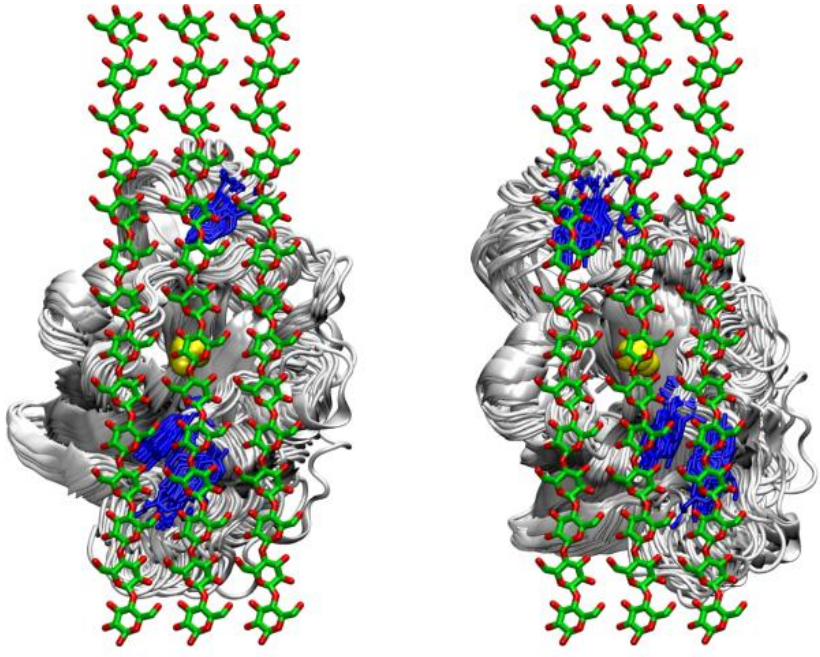

Figure 18. Two unique binding scenarios of *Hi*LPMO9B on cellulose Iβ observed in MD simulation trajectory. Each of the bind modes is demonstrated as clusters of simulation snapshots. The Left panel shows the equilibration mode, in which the three surface-exposed tyrosine residues (Tyr-20, Tyr-36 andTyr-207, shown in blue) were observed to be aligned on the same cellulose chains (green). The right panels shows the rotated mode, where the three tyrosine residues (blue) are positioned across three adjacent cellulose chains (green). The active-site Cu is shown as yellow ball, and the enzyme structure is shown as white grey cartoon.

In contrast to a relatively even contribution between three surface tyrosine residues of *Pc*LPMO9D in substrate binding (Wu *et al.*, 2013), the tyrosine residues on L2 (Tyr-20) and LC loop (Tyr-207) appeared to contribute much more than Tyr-36 (L3 loop) to the substrate binding of *Hi*LPMO9B in terms of interaction energy (Figure 19). In addition, considerable contributions come from the two acidic residues (Asp-205 and Glu-201) on the LC loop in proximity of the conserved LC tyrosine (Tyr-207), whereas there are no acidic residues on the correspond position in

*Pc*LPMO9D molecule. The residues Asp-205 and Glu-201 of *Hi*LPMO9B are found to be involved in hydrogen binding with the glucose moiety in both the equilibration and rotated mode (Figure 20). The side-chain carboxyl group of Glu-210 was observed to interact with the C6- hydroxyl group of glucose through forming direct hydrogen bonding. The indirect hydrogen bonding between Asp-205 and the C6- hydroxyl groups of the substrate occurs via a water molecule (Figure 20).

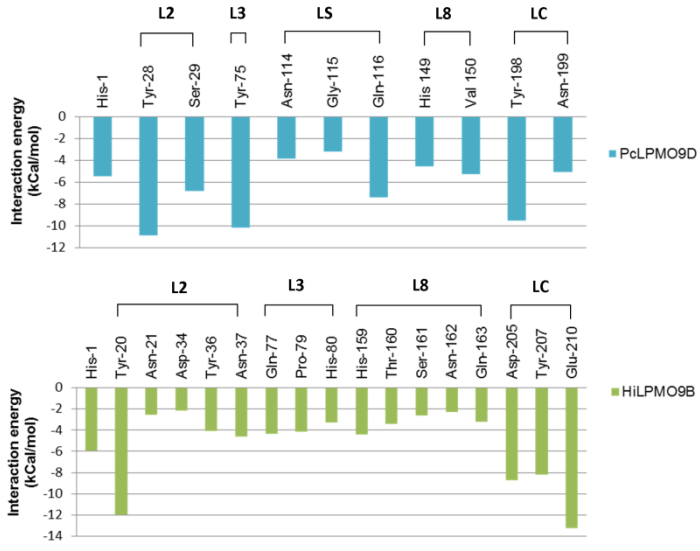

Figure 19. Contribution of substrate interacting residues in *Pc*LPMO9D (Wu *et al*., 2013) and *Hi*LPMO9B (Paper III). The contribution of substrate binding is shown in the total interaction energy (van der Waals plus electrostatic contribution). The corresponding loop regions (L2, L3, LS, L8 and LC) comprising the substrate interacting residues are indicated.

The contribution of the LC loops to substrate interaction is also different between *Hi*LPMO9B and *Pc*LPMO9D. In *Hi*LPMO9B, the two acidic residues (Glu-210 and Asp-205) were found to contribute significantly to the substrate binding (Figure 19). Asp-205 showed a contribution equivalent to Tyr-207 in terms of the average interaction energy, and Glu-210 was found to be the residue giving the strongest substrate interaction, compared to the other substrate interacting residues. *Pc*LPMO9D contains two asparagine residues; Asn-196 and Asn-199, located close the LC-loop

tyrosine (Tyr-198) (Figure 17). Only Asn-199 was shown to be involved the *Pc*LPMO9D-cellulose interaction, with less contribution in substrate binding energy compared to Tyr-198 residues (Wu *et al.*, 2013). By comparison with other C1-specific LPMOs like *Pc*LPMO9D, *Nc*LPMO9F and *Tt*LPMO9E, it is therefore possible that the LC loop of *Hi*LPMO9B participates in other types of interactions than hydrophobic interaction (e.g., hydrogen bonding) to compensate for the absence of substrate interacting residue on the other surface-exposed loops, such as the lack of tyrosine residues on the L3 loop of *Hi*LPMO9B.

Both *Mt*LPMO9G and *Hi*LPMO9B possess an extended L2 loop with two aromatic surface-exposed residues, and both of them lack the conserved tyrosine residue on loop L3. *Mt*LPMO9G also lacks the highly conserved surface-exposed tyrosine of the LC loop (Figure 17). These structural features suggest the extension of loop L2, with multiple surface-exposed hydrophobic residues, could be important for substrate binding in certain C1-specific AA9 LPMOs. These features may suggest an evolutionary adoption of C1-specific LPMO in substrate binding.

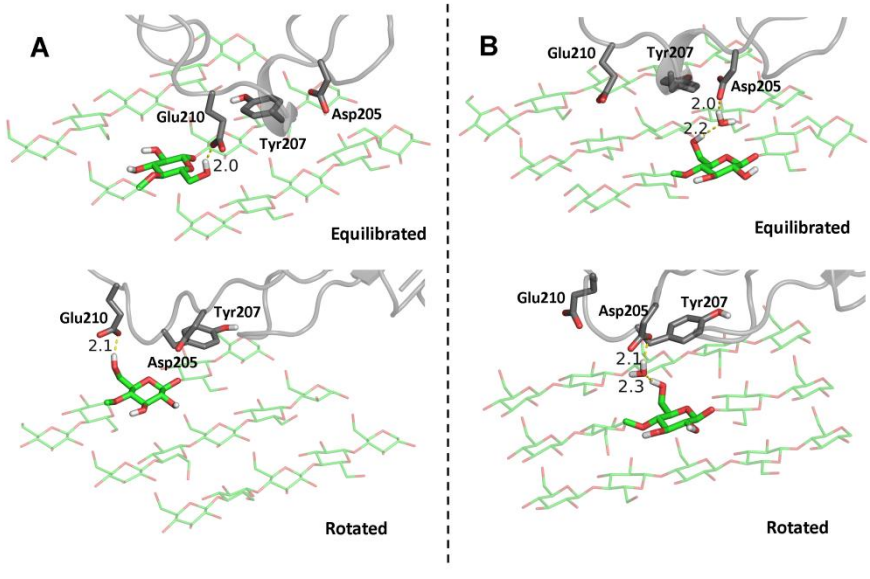

Figure 20. Hydrogen bonding interaction between glucose moieties (green) on cellulose surface and two acidic residues Glu210 (**A**) and Asp 205 (**B**) on the LC loop of *Hi*LPMO9B (dark grey) in equilibrated and rotated binding modes.

Current studies have proposed different cellulose binding scenarios are proposed depending on the substrate preference of AA9 LPMOs. One scenario demonstrated that LPMOs which are only active on insoluble cellulose stacking over the cellulose surface preliminary via hydrophobic interaction between aromatic residues of the LPMO and the glucose rings in cellulose chains (Wu *et al.*, 2013). It has been also revealed that the substrate binding of those LPMOs could be further supported by direct or water-meditated hydrogen bonding between acidic residues of the LPMO and the hydroxyl group of C6 carbon of the surface-exposed sugar ring (Paper III). The other scenario was shown using LPMOs active on both insoluble cellulose and short soluble cellodextrins, in which the substrate interaction is supported by hydrogen bonding between the residues on the unique extension of L3 or L8 loop with the C2 and C3 on the sugar ring (Frandsen *et al.*, 2016; Simmons *et al.*, 2017), in addition to the hydrophobic interaction. Given the morphology of cellulose matrix, it appears that the first-type interaction could target the hydrophobic surface of cellulose microfibrils, where only the ring surface and C6 of glucose moieties are accessible but on the other hand there is relatively large interaction area accessible. While the second-type LPMOs appear to target to the hydrophilic edges of cellulose microfibrils, where there is limited interaction area but the C2 and C3 are more exposed to the environment. The second-type LPMOs could target to the disassociated chains where all side chains are free from the interaction with the neighboring chains. The common activity on cellulose of all characterized AA9 LPMOs and structural diversity may indicate a possible cooperation between different types of AA9 LPMOs contributing to efficient cellulose degradation.

2.1.4 Possible scenarios of Cu-ROS incorporation

Cyanide (CN^-) is known as a copper-binding analog of superoxide ion (Paci *et al.*, 1988). The biochemical effects of cyanide on the activity of *Pc*LPMO9D revealed that CN^- inhibits the AA9 activity on cellulose by competition with O_2 binding to the enzyme (Paper IV), which is similar to the results of a previous study that CN^- inhibits the chitin-degrading activity of an AA10 LPMO (Vaaje-Kolstad *et al.*, 2010). CN^- showed inhibitory effects on the initial rate of *Pc*LMO9D activity degrading crystalline cellulose (Avicel), and the inhibition of enzyme activity by CN^- is independent on the choice of electron donor. A high excess of cyanide (1000 fold over enzyme dosage) showed considerable inhibition of the O_2 composition of *Pc*LPMO9D in absence of substrate. This suggests that the inhibition on AA9 LPMO activity is due to the inhibition of CN^- the reactivity of catalytic Cu with O_2, most likely by the competition of copper binding with O_2 (Paper IV).

The structure of *Pc*LPMO9D in complex with CN^- was solved at 1.8 Å resolution by X-ray crystallography. The CN^- ligand was found to bind to the active-site copper at the axial position at a distance of 2.4 Å, and the occupancy of the modeled CN^- ligand was estimated to be 75% based on the calculated electron density map. The horizontal coordination site of the catalytic Cu is occupied by a water molecule with 25% occupancy (Figure 21A). There was no product formed when *Pc*LPMO9D was incubated with crystalline cellulose with only CN^- present (no reducing agent), indicating that CN^- alone cannot reduce the copper and initiate the redox cycle of the *Pc*LPMO9D's biocatalysis (Paper IV). It further suggests that the active site of *Pc*LPMO9D-CN^- structure crystalized in a reductant-free condition is most likely to be a Cu(II)-CN^- complex, which can be seen as an analog to Cu(II)-superoxyl intermediate (Cu(II)-O_2^-). The coordination of Cu(II)-O_2^- intermediate has been described as "T-brace" where Cu is coordinated by only two active-site residues (two histine residues) and the bound ROS and loses the coordination from the axial-side tyrosine (Kim *et al.*, 2014). Although the crystal structure shows that the Cu of *Pc*LPMO9D was coordinated by three active-site residues (His-1, His-76 and Tyr-176), it can be explained by that the solved *Pc*LPMO9D-CN^- complex reflects a mixture of both CN^--bounded (major) and non-bounded (minor) states, supported by the partial occupancy of ligands observed. Similarly, the partial occupation of ligands around Cu center of AA9 LPMO has also been observed in a previously solved Cu(II)-peroxide (Cu(II)-O_2^{2-}) complex

of the C4-specific *Nc*LPMO9D, showing the formation of Cu (II)-peroxide (59% occupancy) is associated with a reduced occupancy (48%) of an axial water (Figure 21C) (O'Dell *et al.*, 2017).

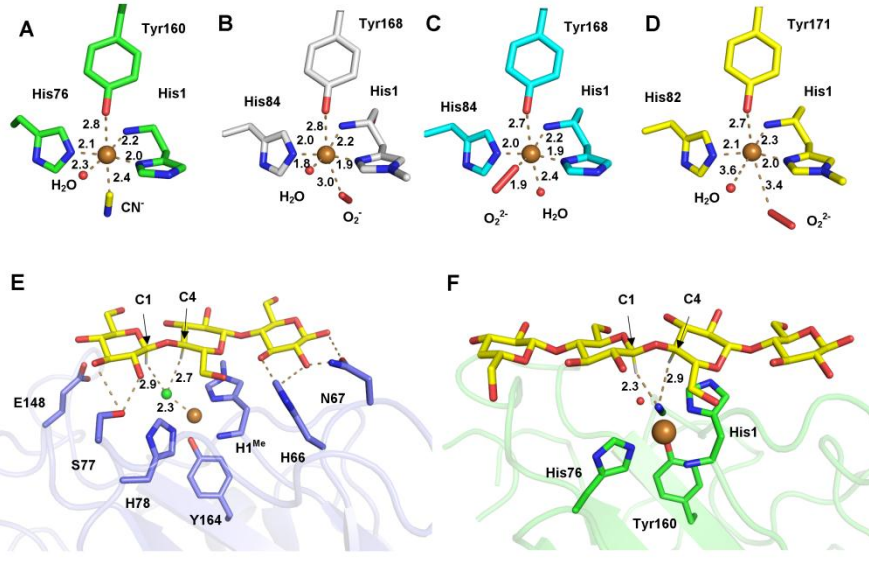

Figure 21. Various crystal structures of AA9 LPMOs in complex with ROS, cyanide, and polysaccharide substrate. (**A**) *Pc*LPMO9D-Cu(II)-CN^- (Paper IV), (B) *Nc*LPMO9D-Cu(II)-O_2^- (PDB: 4EIR), (**C**) *Nc*LPMO9D-Cu(II)-O_2^{2-} (PDB: 5TKH), (**D**) *Nc*LPMO9M-Cu(II)-O_2^{2-} (PDB: 4EIS), (**E**) *Ls*LPMO9A-Cu(II) in complex with cellotriose (PDB: 5ACF), (**F**) superposition of the *Pc*LPMO9D-Cu(II)-CN^- structure to the previous computationally simulated *Pc*LPMO9D in the binding equilibrium of cellulose chains described by Wu *et al.*, (2013). The distance between atoms are measured in Å

The current experimental findings showed diverse scenarios of AA9 structures bound with different ROS ligands or analogs (*Figure 21*). The formation of a Cu (II)-superoxyl (Cu(II)-O_2^-) complex is thought to be the initial step when the catalytic copper is activation by O_2 (Kim *et al.*, 2014; Walton & Davies, 2016). It had previously been reported that a superoxide (O_2^-) was observed on the axial side of the catalytic center of the C4-specific *Nc*LPMO9D in the absence of a bound substrate, though the distance between Cu and O_2^- is a bit too far to be regarded as reactive intermediate (Figure 21B) (Li *et al.*, 2012). The Cu (II)-peroxyl (Cu(II)-O_2^{2-}) complexes of AA9 LPMO structures have also been reported, give that superoxide dissociated from Cu (II) and oxidized to peroxide in the

absence of substrate (Kittl *et al.*, 2012). A peroxide ligand was found to occupy at the axial position in the C1/C4-active *Nc*LPMO9M structure (Figure 21D). A later study revealed that the peroxide ligand was formed from O_2 at the horizontal corner of the copper coordination plane of the C4-specific *Nc*LPMO9D (Figure 21C). Later studies also revealed that some AA9 LPMOs can use H_2O_2 as co-substrate. A new possible reaction pathway has been proposed that Cu(II)-oxyl intermediate is formed directly after the peroxide activates Cu (I) accompanied with external electron donation, whereas Cu(II)-oxyl intermediate is thought to derive from the Cu(II)-superoxyl complex in the O_2-based mechanism (Bissaro *et al.*, 2017). However, neither Cu(I)-superoxyl nor Cu(II)-oxyl complex structure have been observed in current crystallographic results of AA9 LPMOs. Recent studies have pointed out that it gave more reliable indication on the catalytic mechanism when both substrate and ROS ligand/analog are present in the crystal structures of AA9 LPMOs. *Ls*LPMOA is characterized to cleave cello-oligosaccharides using a solely C4-oxdizing mechniasm, but it can degrade insoluble cellulose by oxidizing both C1 and C4. It has been shown that a chloride ion (Cl^-), a mimic of a negatively charged dioxygen species, mediate substrate binding in the *Ls*LPMOA structure in complex with a range of different glycan substrates (Frandsen *et al.*, 2016; Simmons *et al.*, 2017). In all cases, the chloride ion was found occupying the equatorial corner of the Cu active site of this protein in contact with the hydroxyl groups of the substrates, which was thought to mimic the binding of superoxide during catalysis (Figure 21E). It was thought in that case that the equatorial corner is a reasonable O_2 binding position for *Ls*LPMOA, as it is much closer to a highly conserved histidine residue on loop L8 (His-147) and could be a potential agent for the deprotonation of Cu(II)-superoxyl to Cu(II)-oxyl, which is expected to trigger the oxidation of substrate (Frandsen *et al.*, 2016; Simmons *et al.*, 2017).

The C1-specific *Pc*LPMO9D has been reported to only show activity against insoluble cellulose so far. Thus, it is difficult to obtain the structural complex of *Pc*LPMO9D with both substrate and CN^- ligand by crystallographic approaches. In contrast to the crystallographic results of AA9 LPMOs binding to soluble substrates (Frandsen *et al.*, 2016; Simmons *et al.*, 2017), several studies by computational simulations, including paper III, have suggested that $C1^-$specific LPMOs are more likely to sit above the cellulose surface, making the axial position of copper coordinating sites more exposed to the substrate (Wu *et al.*, 2013; Kim *et al.*, 2014).

Interestingly, when superimposing *Pc*LPMO9D-CN^- complex structure onto the modeled structure of *Pc*LPMO9D with cellulose chains from a previous study by Wu *et al*., (2013), the CN^- ligand is found to skew towards the hydrogen on C1 carbon (H1) of the potential scissile bonds in the ligand (Figure 21F), which is in line with the determined C1 oxidized preference of *Pc*LPMO9D. Together with the experimental evidences that CN^- inhibits the catalytic activity of *Pc*LPMO9D and competes with O_2 binding to *Pc*LPMO9D, the *Pc*LPMO9D-CN^- complex structure could provide a possible scenario where the CN^- blocks the access of Cu to O_2, reflecting a mimic of the Cu(II)-superoxyl intermediate in cases of C1-specific LPMOs. The current findings suggest that there might be diverse scenarios for ROS binding depending on the types of LPMOs and ROS used.

3 Conclusions

Two CBM1-containing AA9 LPMO's from the white-rot fungus *H. irregulare* differ in substrate specificity against cellulose and hemicellulose. *Hi*LPMO9H is only active against cellulose while *Hi*LPMO9I shows activity against both cellulose and glucomannan. This indicates that AA9 LPMOs are most likely to be involved in the degradation of both cellulose and hemicellulose during the decay of softwood by *H. irregulare* (Paper I).

*Hi*LPMO9B and *Hi*Cel7A showed cooperation in degradation of crystalline cellulose. *Hi*LPMO9B showed strong ability to degrade crystalline cellulose and also increased substrate accessibility for *Hi*Cel7A to crystalline cellulose. This suggests that AA9 LPMOs could be important components of the cellulose degradation system of *H. irregulare*, and potentially act in synergy with other cellulases (Paper II).

In addition to hydrophobic interaction contributed from aromatic residues, the binding of C1-specific AA9 LPMOs onto cellulose surface could be further explained by direct or water-meditated hydrogen bonding between acidic residues and the hydroxyl group of C6 carbon of glucose unit (Paper III).

Cyanide was shown to compete the binding of O_2 to the C1-specific *Pc*LPMO9D. The structure complex where CN^- occupies the axial position of copper coordinating sites provides a possible scenario mimicking the initial Cu (II)-superoxyl intermediate of C1-specific AA9 LPMOs based on the proposed mechanism using O_2 (Paper IV).

4 Future perspectives

The roles of AA9 LPMO in lignocellulose degradation of *H. irregulare* need to be further investigated at biological level. Knock-out experiments of AA9 genes could be performed to examine whether the fungus suffers from the deficiency in utilization of a certain lignocellulosic substrate, but this will require the development of a method for precise genome editing in *H. irregulare*. Additionally, the contribution of LPMOs to *H. irregulare* colonization of wood can be investigated using advanced microscopic techniques to understand the preference of individual LPMOs on the types of cells or tissues of woody materials. Future works to characterize AA14 LPMOs are required to explore contribution of LPMOs in xylan degradation of *H. irregulare*. Proteomic studies of *H. irregulare* are recommended to spot out potential synergetic partners with LPMOs (both AA9 and AA14) in the degradation of different substrates. Possible combinations of enzyme candidates can be thus tested on natural lignocellulosic substrates to further explore the enzyme machinery of *H. irregulare*

Future structural studies using crystallographic approaches should be applied to LPMOs showing activity against soluble substrates to investigate the residues important for substrate binding and to provide more detailed pictures of LPMO-ROS-substrate complexes. Structural characterization by X-ray absorption spectroscopy can be employed to verify the geometric coordination between the catalytic Cu and ROS ligand in presence of soluble substrate. More MD simulations can be conducted to investigate how different *H. irregulare* LPMOs binds with different types of substrates. The importance of potential substrate binding residues can be investigated

by mutagenesis experiments, followed by assays for binding affinity and catalytic activity. A biochemical assay that enables absolute quantification through tracking the generation of oxidized ends by LPMO is also possible to be developed using solid-state NMR.

References

Agger, J.W., Isaksen, T., Várnai, A., Vidal-Melgosa, S., Willats, W.G.T., Ludwig, R., Horn, S.J., Eijsink, V.G.H. & Westereng, B. (2014). Discovery of LPMO activity on hemicelluloses shows the importance of oxidative processes in plant cell wall degradation. *Proceedings of the National Academy of Sciences of the United States of America*, vol. 111 (17), pp. 6287–6292.

Arantes, V. & Saddler, J.N. (2010). Access to cellulose limits the efficiency of enzymatic hydrolysis: the role of amorphogenesis. *Biotechnology for biofuels*, vol. 3, p. 4.

Asiegbu, F.O., Adomas, A. & Stenlid, J. (2005). Conifer root and butt rot caused by *Heterobasidion annosum (Fr.) Bref. s.l . Molecular Plant Pathology*, vol. 6 (4), pp. 395–409.

Bagley, S.T. & Richter, D.L. (2002). Biodegradation by Brown Rot Fungi. In: Osiewacz, H.D. (ed) *Industrial Applications*. Berlin, Heidelberg: Springer Berlin Heidelberg, pp. 327–341.

Bar-On, Y.M., Phillips, R. & Milo, R. (2018). The biomass distribution on Earth. *Proceedings of the National Academy of Sciences*, p. 201711842.

Beeson, W.T., Phillips, C.M., Cate, J.H.D. & Marletta, M.A. (2012). Oxidative cleavage of cellulose by fungal copper-dependent polysaccharide monooxygenases. *Journal of the American Chemical Society*, vol. 134 (2), pp. 890–892.

Beeson, W.T., Vu, V.V., Span, E.A., Phillips, C.M. & Marletta, M.A. (2015). Cellulose degradation by polysaccharide monooxygenases. *Annual Review of Biochemistry*, vol. 84, pp. 923–946.

Bennati-Granier, C., Garajova, S., Champion, C., Grisel, S., Haon, M., Zhou, S., Fanuel, M., Ropartz, D., Rogniaux, H., Gimbert, I., Record, E. & Berrin, J.-G. (2015). Substrate specificity and regioselectivity of fungal AA9 lytic polysaccharide monooxygenases secreted by *Podospora anserina* . *Biotechnology for Biofuels*, vol. 8, p. 90.

Bissaro, B., Røhr, Å.K., Müller, G., Chylenski, P., Skaugen, M., Forsberg, Z., Horn, S.J., Vaaje-Kolstad, G. & Eijsink, V.G.H. (2017). Oxidative cleavage of polysaccharides by monocopper enzymes depends on H_2O_2. *Nature Chemical Biology*, vol. 13 (10), pp. 1123–1128.

Book, A.J., Yennamalli, R.M., Takasuka, T.E., Currie, C.R., Phillips, G.N. & Fox, B.G. (2014). Evolution of substrate specificity in bacterial AA10 lytic polysaccharide monooxygenases. *Biotechnology for Biofuels*, vol. 7, p. 109.

Brett, C.T. (2000). Cellulose microfibrils in plants: biosynthesis, deposition, and integration into the cell wall. *International Review of Cytology*, vol. 199, pp. 161–199.

Capretti, P., Korhonen, K., Mugnai, L. & Romagnoli, C. (1990). An intersterility group of *Heterobasidion annosum* specialized to *Abies alba* . *European Journal of Forest Pathology*, vol. 20 (4), pp. 231–240.

Chase, T.E. & Ullrich, R.C. (1988). *Heterobasidion annosum* , root- and butt-rot of trees. *Advances in Plant Pathology*, vol. 6, pp. 501–510 (Genetics of Plant Pathogenic Fungi).

Cosgrove, D.J. (1998). Cell Wall Loosening by Expansins. *Plant Physiology*, vol. 118 (2), pp. 333–339.

Courtade, G., Wimmer, R., Røhr, Å.K., Preims, M., Felice, A.K.G., Dimarogona, M., Vaaje-Kolstad, G., Sørlie, M., Sandgren, M., Ludwig, R., Eijsink, V.G.H. & Aachmann, F.L. (2016). Interactions of a fungal lytic polysaccharide monooxygenase with β-glucan substrates and cellobiose dehydrogenase. *Proceedings of the National Academy of Sciences of the United States of America*, vol. 113 (21), pp. 5922–5927.

Couturier, M., Ladevèze, S., Sulzenbacher, G., Ciano, L., Fanuel, M., Moreau, C., Villares, A., Cathala, B., Chaspoul, F., Frandsen, K.E., Labourel, A., Herpoël-Gimbert, I., Grisel, S., Haon, M., Lenfant, N., Rogniaux, H., Ropartz, D., Davies, G.J., Rosso, M.-N., Walton, P.H., Henrissat, B. & Berrin, J.-G. (2018). Lytic xylan oxidases from wood-decay fungi unlock biomass degradation. *Nature Chemical Biology*, vol. 14 (3), pp. 306–310.

Cragg, S.M., Beckham, G.T., Bruce, N.C., Bugg, T.D., Distel, D.L., Dupree, P., Etxabe, A.G., Goodell, B.S., Jellison, J., McGeehan, J.E., McQueen-Mason, S.J., Schnorr, K., Walton, P.H., Watts, J.E. & Zimmer, M. (2015). Lignocellulose degradation mechanisms across the Tree of Life. *Current Opinion in Chemical Biology*, vol. 29, pp. 108–119 (Energy • Mechanistic biology).

Eibinger, M., Ganner, T., Bubner, P., Rošker, S., Kracher, D., Haltrich, D., Ludwig, R., Plank, H. & Nidetzky, B. (2014). Cellulose surface degradation by a lytic polysaccharide monooxygenase and its effect on cellulase hydrolytic efficiency. *The Journal of Biological Chemistry*, vol. 289 (52), pp. 35929–35938.

Eibinger, M., Sattelkow, J., Ganner, T., Plank, H. & Nidetzky, B. (2017). Single-molecule study of oxidative enzymatic deconstruction of cellulose. *Nature Communications*, vol. 8 (1), p. 894.

Feofilova, E.P. & Mysyakina, I.S. (2016). Lignin: Chemical structure, biodegradation, and practical application (a review). *Applied Biochemistry and Microbiology*, vol. 52 (6), pp. 573–581.

Forsberg, Z., Vaaje-Kolstad, G., Westereng, B., Bunæs, A.C., Stenstrøm, Y., MacKenzie, A., Sørlie, M., Horn, S.J. & Eijsink, V.G. (2011). Cleavage of cellulose by a CBM33 protein. *Protein Science : A Publication of the Protein Society*, vol. 20 (9), pp. 1479–1483.

Foster, C.E., Martin, T.M. & Pauly, M. (2010). Comprehensive Compositional Analysis of Plant Cell Walls (Lignocellulosic biomass) Part II: Carbohydrates. *Journal of Visualized Experiments : JoVE*, (37). DOI: https://doi.org/10.3791/1837.

Frandsen, K.E.H., Simmons, T.J., Dupree, P., Poulsen, J.-C.N., Hemsworth, G.R., Ciano, L., Johnston, E.M., Tovborg, M., Johansen, K.S., von Freiesleben, P., Marmuse, L., Fort, S., Cottaz, S., Driguez, H., Henrissat, B., Lenfant, N., Tuna, F., Baldansuren, A., Davies, G.J., Lo Leggio, L. & Walton, P.H. (2016). The molecular basis of polysaccharide cleavage by lytic polysaccharide monooxygenases. *Nature Chemical Biology*, vol. 12 (4), pp. 298–303.

Frommhagen, M., Koetsier, M.J., Westphal, A.H., Visser, J., Hinz, S.W.A., Vincken, J.-P., van Berkel, W.J.H., Kabel, M.A. & Gruppen, H. (2016). Lytic polysaccharide monooxygenases from Myceliophthora thermophila C1 differ in substrate preference and reducing agent specificity. *Biotechnology for Biofuels*, vol. 9 (1), p. 186.

Frommhagen, M., Sforza, S., Westphal, A.H., Visser, J., Hinz, S.W.A., Koetsier, M.J., van Berkel, W.J.H., Gruppen, H. & Kabel, M.A. (2015). Discovery of the combined oxidative cleavage of plant xylan and cellulose by a new fungal polysaccharide monooxygenase. *Biotechnology for Biofuels*, vol. 8, p. 101.

Frommhagen, M., Westphal, A.H., Berkel, V., H, W.J. & Kabel, M.A. (2018). Distinct Substrate Specificities and Electron-Donating Systems of Fungal Lytic Polysaccharide Monooxygenases. *Frontiers in Microbiology*, vol. 9. DOI: https://doi.org/10.3389/fmicb.2018.01080.

Garbelotto, M. & Gonthier, P. (2013). Biology, Epidemiology, and Control of *Heterobasidion* Species Worldwide. *Annual Review of Phytopathology*, vol. 51 (1), pp. 39–59.

Goodell, B., Qian, Y. & Jellison, J. (2008). Fungal Decay of Wood: Soft Rot—Brown Rot—White Rot. *Development of Commercial Wood Preservatives*. (982). American Chemical Society, pp. 9–31.

Guerriero, G., Hausman, J.-F., Strauss, J., Ertan, H. & Siddiqui, K.S. (2015). Destructuring plant biomass: Focus on fungal and extremophilic cell wall hydrolases. *Plant science : an international journal of experimental plant biology*, vol. 234, pp. 180–193.

Guo, Z., Duquesne, S., Bozonnet, S., Nicaud, J.-M., Marty, A. & O'Donohue, M.J. (2017). Expressing accessory proteins in cellulolytic *Yarrowia lipolytica* to improve the conversion yield of recalcitrant cellulose. *Biotechnology for Biofuels*, vol. 10, p. 298.

Hall, M., Bansal, P., Lee, J.H., Realff, M.J. & Bommarius, A.S. (2010). Cellulose crystallinity – a key predictor of the enzymatic hydrolysis rate. *FEBS Journal*, vol. 277 (6), pp. 1571–1582.

Harris, P.V., Welner, D., McFarland, K.C., Re, E., Navarro Poulsen, J.-C., Brown, K., Salbo, R., Ding, H., Vlasenko, E., Merino, S., Xu, F., Cherry, J., Larsen, S. & Lo Leggio, L. (2010). Stimulation of lignocellulosic biomass hydrolysis by proteins of glycoside hydrolase family 61: structure and function of a large, enigmatic family. *Biochemistry*, vol. 49 (15), pp. 3305–3316.

Hemsworth, G.R., Davies, G.J. & Walton, P.H. (2013). Recent insights into copper-containing lytic polysaccharide mono-oxygenases. *Current opinion in structural biology*, vol. 23 (5), pp. 660–668.

Hemsworth, G.R., Henrissat, B., Davies, G.J. & Walton, P.H. (2014). Discovery and characterization of a new family of lytic polysaccharide mono-oxygenases. *Nature chemical biology*, vol. 10 (2), pp. 122–126.

Hemsworth, G.R., Johnston, E.M., Davies, G.J. & Walton, P.H. (2015). Lytic polysaccharide monooxygenases in biomass conversion. *Trends in Biotechnology*, vol. 33 (12), pp. 747–761.

Horn, S.J., Vaaje-Kolstad, G., Westereng, B. & Eijsink, V.G. (2012). Novel enzymes for the degradation of cellulose. *Biotechnology for biofuels*, vol. 5 (1), p. 45.

Isaksen, T., Westereng, B., Aachmann, F.L., Agger, J.W., Kracher, D., Kittl, R., Ludwig, R., Haltrich, D., Eijsink, V.G.H. & Horn, S.J. (2014). A C4-oxidizing lytic polysaccharide monooxygenase cleaving both cellulose and cello-oligosaccharides. *The Journal of biological chemistry*, vol. 289 (5), pp. 2632–2642.

Jaramillo, P.M.D., Gomes, H.A.R., Monclaro, A.V., Silva, C.O.G. & Filho, E.X.F. (2015). Lignocellulose-degrading enzymes. *Fungal Biomolecules*. Wiley-Blackwell, pp. 73–85.

Jung, S., Song, Y., Kim, H.M. & Bae, H.-J. (2015). Enhanced lignocellulosic biomass hydrolysis by oxidative lytic polysaccharide monooxygenases (LPMOs) GH61 from *Gloeophyllum trabeum*. *Enzyme and Microbial Technology*, vol. 77, pp. 38–45.

Karkehabadi, S., Hansson, H., Kim, S., Piens, K., Mitchinson, C. & Sandgren, M. (2008). The first structure of a glycoside hydrolase family 61 member, Cel61B from *Hypocrea jecorina*, at 1.6 A resolution. *Journal of molecular biology*, vol. 383 (1), pp. 144–154.

Kim, S., Ståhlberg, J., Sandgren, M., Paton, R.S. & Beckham, G.T. (2014). Quantum mechanical calculations suggest that lytic polysaccharide monooxygenases use a copper-oxyl, oxygen-rebound mechanism. *Proceedings of the National Academy of Sciences of the United States of America*, vol. 111 (1), pp. 149–154.

Kittl, R., Kracher, D., Burgstaller, D., Haltrich, D. & Ludwig, R. (2012). Production of four *Neurospora crassa* lytic polysaccharide monooxygenases in *Pichia pastoris* monitored by a fluorimetric assay. *Biotechnology for Biofuels*, vol. 5 (1), p. 79.

Kojima, Y., Várnai, A., Ishida, T., Sunagawa, N., Petrovic, D.M., Igarashi, K., Jellison, J., Goodell, B., Alfredsen, G., Westereng, B., Eijsink, V.G.H. & Yoshida, M. (2016). A Lytic Polysaccharide Monooxygenase with Broad Xyloglucan Specificity from the Brown-Rot Fungus *Gloeophyllum trabeum* and Its Action on Cellulose-Xyloglucan Complexes. *Applied and Environmental Microbiology*, vol. 82 (22), pp. 6557–6572.

Kont, R., Kari, J., Borch, K., Westh, P. & Väljamäe, P. (2016). Inter-domain Synergism Is Required for Efficient Feeding of Cellulose Chain into Active Site of Cellobiohydrolase Cel7A. *The Journal of Biological Chemistry*, vol. 291 (50), pp. 26013–26023.

Korhonen, K. (1978). Intersterility groups of *Heterobasidion annosum*. *Communicationes Instituti Forestalis Fenniae*, vol. 94, p. 25.

Kuhad, R.C., Gupta, R. & Singh, A. *Microbial Cellulases and Their Industrial Applications*. (2011) (Enzyme Research). DOI: https://doi.org/10.4061/2011/280696.

Langston, J.A., Shaghasi, T., Abbate, E., Xu, F., Vlasenko, E. & Sweeney, M.D. (2011). Oxidoreductive cellulose depolymerization by the enzymes cellobiose dehydrogenase and glycoside hydrolase 61. *Applied and environmental microbiology*, vol. 77 (19), pp. 7007–7015.

Leggio, L.L., Simmons, T.J., Poulsen, J.-C.N., Frandsen, K.E.H., Hemsworth, G.R., Stringer, M.A., Freiesleben, P. von, Tovborg, M., Johansen, K.S., Maria, L.D., Harris, P.V., Soong, C.-L., Dupree, P., Tryfona, T., Lenfant, N., Henrissat, B., Davies, G.J. & Walton, P.H. (2015). Structure and boosting activity of a starch-degrading lytic polysaccharide monooxygenase. *Nature Communications*, vol. 6, p. 5961.

Leggio, L.L., Welner, D. & De Maria, L. (2012). A structural overview of GH61 proteins - fungal cellulose degrading polysaccharide monooxygenases. *Computational and structural biotechnology journal*, vol. 2, p. e201209019.

Levy, J. (1966). The Soft Rot Fungi: Their Mode of Action and Significance in the Degradation of Wood. In: Preston, R.D. (ed) *Advances in Botanical Research*. Academic Press, pp. 323–357.

Li, X., Beeson, W.T., 4th, Phillips, C.M., Marletta, M.A. & Cate, J.H.D. (2012). Structural basis for substrate targeting and catalysis by fungal polysaccharide monooxygenases. *Structure (London, England: 1993)*, vol. 20 (6), pp. 1051–1061.

Lind, M., Stenlid, J. & Olson, Å. (2014). Chapter Twelve - *Heterobasidion annosum s.l.* Genomics. In: Martin, F.M. (ed) *Advances in Botanical Research*. Academic Press, pp. 371–396.

Lynd, L.R., Weimer, P.J., van Zyl, W.H. & Pretorius, I.S. (2002). Microbial cellulose utilization: fundamentals and biotechnology. *Microbiology and Molecular Biology Reviews*, vol. 66 (3), pp. 506–577.

Mäkelä, M.R., Donofrio, N. & de Vries, R.P. (2014). Plant biomass degradation by fungi. *Fungal Genetics and Biology*, vol. 72 (Supplement C), pp. 2–9 (Biomass Degradation by Fungi).

Mester, T., Varela, E. & Tien, M. (2004). Wood Degradation by Brown-Rot and White-Rot Fungi. In: Kück, U. (ed) *Genetics and Biotechnology*. Berlin, Heidelberg: Springer Berlin Heidelberg, pp. 355–368.

Momeni, M.H., Payne, C.M., Hansson, H., Mikkelsen, N.E., Svedberg, J., Engström, Å., Sandgren, M., Beckham, G.T. & Ståhlberg, J. (2013). Structural, Biochemical, and Computational Characterization of the Glycoside Hydrolase Family 7 Cellobiohydrolase of the Tree-killing Fungus *Heterobasidion irregulare*. *Journal of Biological Chemistry*, vol. 288 (8), pp. 5861–5872.

Moreira, L.R.S. & Filho, E.X.F. (2008). An overview of mannan structure and mannan-degrading enzyme systems. *Applied Microbiology and Biotechnology*, vol. 79 (2), pp. 165–178.

Nekiunaite, L., Petrović, D.M., Westereng, B., Vaaje-Kolstad, G., Hachem, M.A., Várnai, A. & Eijsink, V.G.H. (2016). FgLPMO9A from *Fusarium graminearum* cleaves xyloglucan independently of the backbone substitution pattern. *FEBS letters*, vol. 590 (19), pp. 3346–3356.

Ochoa-Villarreal, M., Aispuro-Hernndez, E., Vargas-Arispuro, I. & ngel, M. (2012). Plant cell wall polymers: function, structure and biological activity of their derivatives. In: De Souza Gomes, A. (ed) *Polymerization*. InTech,.

O'Dell, W.B., Agarwal, P.K. & Meilleur, F. (2017). Oxygen Activation at the Active Site of a Fungal Lytic Polysaccharide Monooxygenase. *Angewandte Chemie International Edition*, vol. 56 (3), pp. 767–770.

Olson, Å., Aerts, A., Asiegbu, F., Belbahri, L., Bouzid, O., Broberg, A., Canbäck, B., Coutinho, P.M., Cullen, D., Dalman, K., Deflorio, G., van Diepen, L.T.A., Dunand, C., Duplessis, S., Durling, M., Gonthier, P., Grimwood, J., Fossdal, C.G., Hansson, D., Henrissat, B., Hietala, A., Himmelstrand, K., Hoffmeister, D., Högberg, N., James, T.Y., Karlsson, M., Kohler, A., Kües, U., Lee, Y.-H., Lin, Y.-C., Lind, M., Lindquist, E., Lombard, V., Lucas, S., Lundén, K., Morin, E., Murat, C., Park, J., Raffaello, T., Rouzé, P., Salamov, A., Schmutz, J., Solheim, H., Ståhlberg, J., Vélëz, H., de Vries, R.P., Wiebenga, A., Woodward, S., Yakovlev, I., Garbelotto, M., Martin, F., Grigoriev, I.V. & Stenlid, J. (2012). Insight into trade-off between wood decay and parasitism from the genome of a fungal forest pathogen. *New Phytologist*, vol. 194 (4), pp. 1001–1013.

Paci, M., Desideri, A. & Rotilio, G. (1988). Cyanide binding to Cu, Zn superoxide dismutase. An NMR study of the Cu(II), Co(II) derivative. *The Journal of Biological Chemistry*, vol. 263 (1), pp. 162–166.

Pierce, B.C., Agger, J.W., Zhang, Z., Wichmann, J. & Meyer, A.S. (2017). A comparative study on the activity of fungal lytic polysaccharide monooxygenases for the depolymerization of cellulose in soybean spent flakes. *Carbohydrate Research*, vol. 449, pp. 85–94.

Quiroz-Castañeda, R.E., Martínez-Anaya, C., Cuervo-Soto, L.I., Segovia, L. & Folch-Mallol, J.L. (2011). Loosenin, a novel protein with cellulose-disrupting activity from Bjerkandera adusta. *Microbial Cell Factories*, vol. 10 (1), p. 8.

Reese, E.T., Siu, R.G.H. & Levinson, H.S. (1950). The biological degradation of soluble cellulose derivatives and its relationship to the mechanism of cellulose hydrolysis. *Journal of Bacteriology*, vol. 59 (4), pp. 485–497.

Sabbadin, F., Hemsworth, G.R., Ciano, L., Henrissat, B., Dupree, P., Tryfona, T., Marques, R.D.S., Sweeney, S.T., Besser, K., Elias, L., Pesante, G., Li, Y., Dowle, A.A., Bates, R., Gomez, L.D., Simister, R., Davies, G.J., Walton, P.H., Bruce, N.C. & McQueen-Mason, S.J. (2018). An ancient family of lytic polysaccharide monooxygenases with roles in arthropod development and biomass digestion. *Nature Communications*, vol. 9 (1), p. 756.

Saha, B.C. & Bothast, R.J. (1999). Enzymology of Xylan Degradation. *Biopolymers*. (723). American Chemical Society, pp. 167–194.

Scheller, H.V. & Ulvskov, P. (2010). Hemicelluloses. *Annual Review of Plant Biology*, vol. 61, pp. 263–289.

Schmidt, O. (2006). *Wood and Tree Fungi: Biology, Damage, Protection, and Use*. Berlin Heidelberg: Springer-Verlag. Available from: //www.springer.com/gp/book/9783540321385. [Accessed 2018-03-12].

Schwarze, F.W.M.R., Engels, J. & Mattheck, C. (2000). *Fungal Strategies of Wood Decay in Trees*. Berlin Heidelberg: Springer-Verlag. Available from: //www.springer.com/us/book/9783642631337. [Accessed 2018-09-24].

Serin, Z., Gümüşkaya, E. & Ondaral, S. (2003). A Review of the Chemical Composition of Different Softwoods, Hardwoods and Annual Plants., September 1 2003.

Simmons, T.J., Frandsen, K.E.H., Ciano, L., Tryfona, T., Lenfant, N., Poulsen, J.C., Wilson, L.F.L., Tandrup, T., Tovborg, M., Schnorr, K., Johansen, K.S., Henrissat, B., Walton, P.H., Lo Leggio, L. & Dupree, P. (2017). Structural and electronic determinants of lytic polysaccharide monooxygenase reactivity on polysaccharide substrates. *Nature Communications*, vol. 8. DOI: https://doi.org/10.1038/s41467-017-01247-3.

Tomme, P., Warren, R.A.J. & Gilkes, N.R. (1995). Cellulose Hydrolysis by Bacteria and Fungi. In: Poole, R.K. (ed) *Advances in Microbial Physiology*. Academic Press, pp. 1–81.

Vaaje-Kolstad, G., Westereng, B., Horn, S.J., Liu, Z., Zhai, H., Sørlie, M. & Eijsink, V.G.H. (2010). An oxidative enzyme boosting the enzymatic conversion of recalcitrant polysaccharides. *Science*, vol. 330 (6001), pp. 219–222.

Vermaas, J.V., Crowley, M.F., Beckham, G.T. & Payne, C.M. (2015). Effects of Lytic Polysaccharide Monooxygenase Oxidation on Cellulose Structure and Binding of Oxidized Cellulose Oligomers to Cellulases. *The Journal of Physical Chemistry B*, vol. 119 (20), pp. 6129–6143.

Villares, A., Moreau, C., Bennati-Granier, C., Garajova, S., Foucat, L., Falourd, X., Saake, B., Berrin, J.-G. & Cathala, B. (2017). Lytic polysaccharide monooxygenases disrupt the cellulose fibers structure. *Scientific Reports*, vol. 7, p. srep40262.

Walker, L.P. & Wilson, D.B. (1991). Enzymatic hydrolysis of cellulose: An overview. *Bioresource Technology*, vol. 36 (1), pp. 3–14 (Enzymatic Hydrolysis of Cellulose).

Walton, P.H. & Davies, G.J. (2016). On the catalytic mechanisms of lytic polysaccharide monooxygenases. *Current Opinion in Chemical Biology*, vol. 31 (Supplement C), pp. 195–207 (Biocatalysis and biotransformation * Bioinorganic chemistry).

Westereng, B., Ishida, T., Vaaje-Kolstad, G., Wu, M., Eijsink, V.G.H., Igarashi, K., Samejima, M., Ståhlberg, J., Horn, S.J. & Sandgren, M. (2011). The Putative Endoglucanase PcGH61D from *Phanerochaete chrysosporium* is a metal-dependent oxidative enzyme that cleaves cellulose. *PLOS ONE*, vol. 6 (11), p. e27807.

Woodward, S., Stenlid, J., Karjalainen, R. & Hüttermann, A. (1998). *Heterobasidion annosum*. biology, ecology, impact and control. *CAB International. Cambridge,*. Available from: http://onlinelibrary.wiley.com/doi/10.1046/j.1365-3059.1999.0366b.x/abstract. [Accessed 2017-05-19].

Wu, M., Beckham, G.T., Larsson, A.M., Ishida, T., Kim, S., Payne, C.M., Himmel, M.E., Crowley, M.F., Horn, S.J., Westereng, B., Igarashi, K., Samejima, M., Ståhlberg, J., Eijsink, V.G.H. & Sandgren, M. (2013). Crystal structure and computational characterization of the lytic polysaccharide monooxygenase GH61D from the Basidiomycota fungus *Phanerochaete chrysosporium*. *The Journal of biological chemistry*, vol. 288 (18), pp. 12828–12839.

Popular science summary

Lignocellulose is the most abundant natural resources on earth, and fungi are natural degraders of lignocellulose biomass using enzymatic approaches. Deciphering the enzyme machinery of fungal systems for lignocellulose degradation will provide better guidance in design of biotechnological applications in biomass conversion to biofuel and valuable products, which further contributes to a sustainable bioeconomy.

Lytic polysaccharide monooxygenases (LPMOs) are oxidative enzymes that cleave recalcitrant polysaccharides using reactive oxygen species (ROS) such as O_2. In order to further dissect the function and catalytic mechanism of LPMOs in fungal systems, I have compared the activity of several fungal LPMOs on different plant cell wall components and have investigated the possible cooperation between LPMOs and cellulases. In addition, I have also studied the possible ways that LPMOs interact with cellulose and how ROS binds to the active site of LPMOs

In summary, the current study support that AA9 LPMOs could be involved in the degradation of both cellulose and hemicellulose during the fungus's degradation on ligocellulosic biomass. AA9 LPMOs may play important role in degradation of crystalline cellulose in synergy with cellulases. The binding of AA9 LPMOs to cellulose are dependent on the structural features of the enzymes, which may involve different types of interactions. The ROS binding to AA9 LPMOs may vary, depending on how the enzymes interact with the substrates. Further studies are still needed to confirm the biological roles of LPMOs and to develop better understanding of structure-function relationship.

Acknowledgements

I am thankful to have a supportive team of supervision: my main supervisor *Mats Sandgren*, who offers me the opportunity for this project, allows me to have great flexibility at work, and provides me strategic guidance in science and personal development; as well as the co-supervisors: *Jerry Ståhlberg* for the inspiration to me with his wide knowledge of enzymology and educative interaction on the art of scientific communication, *Miao Wu* for sharing her skills in laboratorial works and taking care of me like an elder sister at work, *Anders Broberg* from whom I grasped substantial knowledge/skills in analytical chemistry via crash courses and learnt to be more detail-focused and efficient in scientific research, and *Åke Olson* for the open discussion of understanding the secret life of *H. irregulare* and for coaching me how to tell reasonable stories in biology.

I would also like to thank the other "helping hands" at the department of molecular sciences: *Henrik* for kind assistance in analytical instrumentation, *Nils* for being supportive in technical issues, *Saeid* for advices/help in crystallography, *Suresh* and *Jan* for sharing their know-how and valuable tricks in mass spectrometry that I could never learn from the textbooks;

Of course there are other helpful colleagues to thank*: Anja* for being good companion in lab, sharing life experiences at fika and cheering me up with her optimism, *Topi* for being a great teammate in different challenges (coping with failures, fixing troubles, finding way out of forests, manufacturing batches of dumplings…) and giving his hands whenever I needed, *Sumitha* for being well cooperative in project work and encouraging me to keep hoping that the good is yet to come, *Madhu* (my LPMO buddy *below zero*) for our brotherhood with our troublesome LPMOs and encouragement to each other, *Maria* (my previous LPMO

mentor) for giving me the training that enabled me to conduct independent research later on and being a great example of professionalism; *Nisha* for being a supportive co-worker in our LPMO projects; *Benjamin, Johanna, Mikael* for their kind sharing of experimentation expertise in different areas that save me great amount of time, *Marfuz, Jule, Laura, Pernilla* for enjoyable teamship in lab teaching. *Jonas, Mikolaj, Viktoriia* for their positive laughers to neutralize my silence in the office. *Xue* for bringing some balance to my working life at SLU with casual talks.

I also want to express my gratitude to those supporting me behind the scene:

Mom and Dad, thankful for your support with gentle love in silence; *My Chinese friends in distance*, I appreciate for your comfort and encouragement to me on the other side of the line; Aunt Ruyu, thanks for supporting me with your prayers day by day; *Chinese Christian fellowship in Uppsala*, where I feel the sense of family though away from home, and friends in the associated youth group for unforgettable fellowship in personal and spiritual growth; *All the others* that have come into my life during the period, the lovely and precious moments that we have shared are stored deep in my memory. *Pianos* in basements/lunch rooms/churchs for your accompany at numberless nights and being patient listeners to my stories.

爸爸妈妈, 谢谢你们用无声的爱支持我。远方的朋友，感激你们在电话那头的鼓励和安慰。玉姨，很感恩你每天用祷告来支持我。团契的弟兄姊妹，谢谢你们让我在异国他乡也能有家的感受。青年小组的朋友们，感恩有你们在成长路上的陪伴。以及这些年来其他所有曾走进我生活中的人们，那些美好珍贵的记忆都一直留在我内心的深处。还有那些陪伴我度过无数夜晚的钢琴，谢谢你们耐心地听我一遍又一遍讲述我自己的故事。

Thank you, **God**, that you guide me to know better of you, accompany me to grow in your love, carry me through the darkness, and bring me the value and hope of life.

感谢神，一直引导着我更多认识你，陪伴着我在爱中成长，背负着我在黑暗中前行，让我看见人生的价值与盼望。